CHALMERS
UNIVERSITY OF TECHNOLOGY

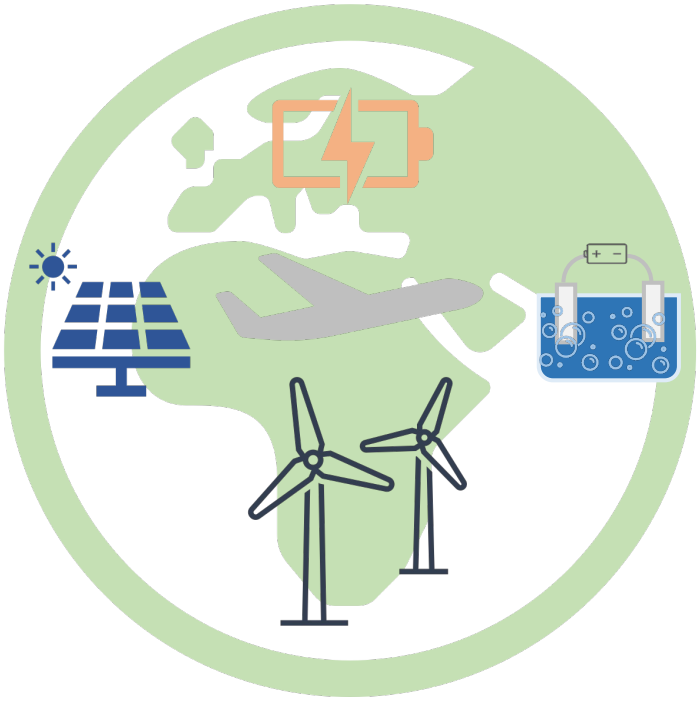

Providing Electricity and Hydrogen as Aviation Fuels

A 2050 Case Study at Göteborg Landvetter Airport

Master's thesis in Sustainable Energy Systems

Arbana Brati & Hanna Pettersson

DEPARTMENT OF SPACE, EARTH AND ENVIRONMENT
CHALMERS UNIVERSITY OF TECHNOLOGY
Gothenburg, Sweden 2024
www.chalmers.se

Master's thesis 2024

Providing Electricity and Hydrogen as Aviation Fuels

A 2050 Case Study at Göteborg Landvetter Airport

Arbana Brati & Hanna Pettersson

CHALMERS
UNIVERSITY OF TECHNOLOGY

Department of Space, Earth and Environment
Division of Energy Technology
Chalmers University of Technology
Gothenburg, Sweden 2024

Providing Electricity and Hydrogen as Aviation Fuels
A 2050 Case Study at Göteborg Landvetter Airport
ARBANA BRATI & HANNA PETTERSSON

Supervisor: Sofia Rosén, Department of Space, Earth, Environment
Examiner: Lisa Göransson, Department of Space, Earth, Environment

Master's Thesis 2024
Department of Space, Earth and Environment
Division of Energy Technology
Chalmers University of Technology
SE-412 96 Gothenburg
Telephone +46 31 772 1000

Cover: A visual representation of electricity and hydrogen production units for electrification of aircraft.

Typeset in LaTeX
Printed by Chalmers Reproservice
Gothenburg, Sweden 2024

Providing Electricity and Hydrogen as Aviation Fuels
A 2050 Case Study at Göteborg Landvetter Airport
ARBANA BRATI & HANNA PETTERSSON
Department of Space, Earth and Environment
Chalmers University of Technology

Abstract

This thesis investigated the direct and indirect electrification of Göteborg Landvetter Airport through the use of battery-electric and hydrogen powered aircraft, where both onsite production and import of green hydrogen and electricity were taken into consideration. More specifically, this thesis investigates how the expected hydrogen and electricity demand could be supplied. Additionally, the key parameters that affect the energy system's behavior were examined by performing a sensitivity analysis. The energy system modeled in GAMS included alkaline water electrolysis, liquefaction, storage of electricity and hydrogen, compression of hydrogen, import of hydrogen through pipeline and trucks and local electricity production via wind power and solar PVs. The results showed that electricity for recharging of aircraft can be supplied at an average marginal cost of 49 €/MWh while gaseous and liquid hydrogen can be supplied at an average marginal cost of 53-54 €/MWh and 74-78 €/MWh respectively. The cost optimal solution always included an electrolyzer located onsite that produced the majority of hydrogen. The total system cost was also found to be highly dependent on local wind power and an increased connection to the electricity grid. Moreover, the hydrogen storage with the largest impact on the total system cost was the cryogenic tank which enables operation at maximum load for the liquefaction plant during more hours of the year.

Keywords: Aviation, Hydrogen, Hydrogen storage, Electrification, Energy system modeling, Linear programming, Liquefaction, Water electrolysis

Acknowledgements

Vi vill tacka alla som har bidragit till detta examensarbete. Först och främst vill vi tacka vår handledare Sofia Rosén som har varit ett stort stöd under examensarbetet och bidragit med insiktsfull feedback och uppmuntran. Vi är djupt tacksamma för den tid du har investerat i oss och att vi alltid har känt oss välkomna att ställa frågor. Vi vill även rikta ett stort tack till vår examinator Lisa Göransson, som har bidragit med värdefull vägledning och expertis gällande energisystem.

Vidare vill vi tacka John Nilsson (Swedavia AB) som bidragit med information gällande el- och vätgasstrategin inom flygindustrin. Ett särskilt tack till Cecilia Andersson (Swedavia AB) som har varit en stor hjälp med kunskap gällande flygplatsdrift och förmedling av rätt kontakter. Vi vill också tacka Niklas Mattson (Chalmers) för hjälpen med modellering i GAMS samt Joel Löfving (Chalmers) för att ha tagit emot vår idé om arbetet och introducerat oss till Sofia.

Slutligen vill vi rikta ett hjärtligt tack till våra familjemedlemmar för deras kärlek och förståelse, och våra vänner från Kf-19, MPSES och exjobbsrummet för deras kontinuerliga stöd och uppmuntran under studietiden.

Arbana Brati & Hanna Pettersson, Göteborg, Juni 2024

List of Acronyms

Below is the list of acronyms that have been used throughout this thesis listed in alphabetical order:

ACA	Airport Carbon Accreditation
AE	Alkaline Water Electrolysis
CEPCI	Chemical Engineering Plant Cost Index
BEA	Battery-Electric Aircraft
DOE	Department of Energy
HDSAM	Hydrogen Delivery Scenario Analysis Model
GAMS	General Algebraic Modeling System
HVO	Hydrotreated Vegetable Oil
LRC	Lined Rock Cavern
LP	Linear Programming
MIP	Mixed Integer Programming
NASA	National Aeronautics and Space Administration
PEM	Proton Exchange Membrane Electrolyzer
PV	Photovoltaic
RHS	Right Hand Side
SAF	Sustainable Aviation Fuel
SMR	Steam Methane Reforming
SOC	State of Charge
SOE	Solid Oxide Electrolyzers

Nomenclature

This section will present the nomenclature of sets, parameters and variables that have been used throughout this thesis.

Sets

T	Set of timesteps, all hours of the year
A	Set of technologies
B	Set of storages
G	Subset of A, containing wind power and solar PV

Parameters

η_{β}^{ch}	Charging efficiency of storage
η_{β}^{disch}	Discharging efficiency of storage
δ_{β}	Hydrogen stand-by losses from storage
γ_{β}^{ch}	Charge rate of storage
γ_{β}^{disch}	Discharge rate of storage
ε	Electricity consumption per unit energy of hydrogen
e	Specific energy
r	Discount rate
a	Annuity factor
C^{CAPEX}	Capital expenditures
C^{VOM}	Variable operational and maintenance cost
C^{FOM}	Fixed operational and maintenance cost
C_t^{el}	Electricity price
C^{H_2}	Hydrogen gas price
$CF_{x,t}$	Capacity factor of electricity generation technologies

D_t^{BEA}	Total electricity demand for charging of BEA
$D_t^{BEA,Fix}$	Fixed electricity demand for charging of BEA
$D_t^{BEA,Flex}$	Flexible electricity demand for charging of BEA
$D_t^{H_2}$	Refueling demand of gaseous hydrogen
$D_t^{LH_2}$	Refueling demand of liquid hydrogen
n^r	Reset profile for flexible night charge
n^a	Availability profile for flexible night charge

Variables

X_t^{el}	Export of electricity
$P_{\alpha,t}$	Produced electricity or hydrogen from technologies
F_t^{BtoLiq}	Feed hydrogen from point B to liquefaction
F_t^{DtoLiq}	Feed hydrogen from point D to liquefaction
F_t^{CtoD}	Hydrogen from point C to D (bypassing LRC)
F_t^{EtoF}	Hydrogen from point E to F (bypassing H_2 tank)
F_t^{GtoH}	Hydrogen from point G to H (bypassing LH_2 tank)
$F_t^{Recirculation}$	Recirculated boil-off sent for liquefaction
Cap_α	Capacity of technologies
Cap_β	Capacity of storage
$SOC_{\beta,t}$	State of charge for storage
$Ch_{\beta,t}$	Charge of storage
$Disch_{\beta,t}$	Discharge of storage
$FlexCh_t$	Charge of flexible load from BEA

Contents

List of Acronyms ix

Nomenclature xi

List of Figures xv

List of Tables xix

1 Introduction 1
- 1.1 Aim . . . 2
- 1.2 Limitations . . . 3

2 Theory 5
- 2.1 Hydrogen for Aviation . . . 5
  - 2.1.1 Water Electrolysis . . . 5
  - 2.1.2 Liquefaction . . . 7
  - 2.1.3 Hydrogen Storage . . . 8
  - 2.1.4 Hydrogen Gas Compression . . . 10
  - 2.1.5 Import of Hydrogen . . . 10
- 2.2 Electricity for Aviation . . . 11
  - 2.2.1 Lithium Batteries . . . 11
  - 2.2.2 Wind and Solar Power in the Airport Environment . . . 12

3 Methods 13
- 3.1 Construction of Demand Profiles . . . 13
  - 3.1.1 Cases . . . 14
- 3.2 Energy System Model . . . 15
  - 3.2.1 Objective Function . . . 17
  - 3.2.2 Electricity Balances . . . 17
    - 3.2.2.1 Flexible Charging . . . 18
  - 3.2.3 Hydrogen Balances . . . 19
- 3.3 Quantitative Data . . . 21
  - 3.3.1 Cost Parameters . . . 21
  - 3.3.2 Technical Parameters . . . 23
  - 3.3.3 Space Requirements . . . 25
  - 3.3.4 Cost of Aviation Fuels . . . 25
- 3.4 Sensitivity Analysis . . . 26

4 Results **27**
4.1 Electricity and Hydrogen Demand 27
4.2 Electricity and Hydrogen Supply 29
4.2.1 Installed Capacity 29
4.2.2 Load Duration Curves 32
4.2.3 Demand and Supply of Electricity 33
4.2.4 State of Charge 34
4.2.5 Space Requirement 35
4.2.6 Cost of Aviation Fuels 36
4.3 Sensitivity Analysis 37
4.3.1 Technology Limitations 37
4.3.2 Varying Key Parameters 41

5 Discussion **43**

6 Conclusion **47**

References **49**

Appendix **I**

A Efficiencies **I**

B Costs: Liquefaction & Cryogenic Tank **III**

C Load Duration Curves **V**

D Sensitivity Analysis: Capacities **VII**
D.1 Single Limitations VII
D.2 Double Limitations IX

E Electricity Supply and Consumption **XIII**

List of Figures

3.1 A visual representation of the energy system including electricity and hydrogen flows, where LH_2 is liquid hydrogen and H_2 is gaseous hydrogen. . . . 15
3.2 The hourly price profile of electricity for year 2050 based on weather data from 2019. . . . 23

4.1 The hourly distance profile for flight range 0-400 km. . . . 28
4.2 The hourly distance profile for flight range 400-800 km. . . . 28
4.3 The hourly distance profile for flight range 800-1500 km. . . . 28
4.4 The hourly distance profile for flight range 1500-3100 km. . . . 29
4.5 The hourly distance profile for flight ranges up to 3100 km for 8 days. 29
4.6 The installed capacities in the cost optimal solution for electrolyzer, liquefaction and compressors expressed in hydrogen output for Case 1, 2 and 3. . . . 30
4.7 The installed capacities in the cost optimal solution for wind power, solar PVs and cable for Case 1, 2 and 3. . . . 30
4.8 The produced and exported electricity in the cost optimal solution for Case 1, 2 and 3. . . . 31
4.9 The installed capacities in the cost optimal solution for LRC, cryogenic tank and the pressurized vessel for Case 1, Case 2 and Case 3. . . . 31
4.10 The load duration for the produced LH_2 from the liquefaction plant. . 32
4.11 The load duration for the produced H_2 from the electrolyzer. . . . 32
4.12 Electricity consumption of different units during 8 days. . . . 33
4.13 Electricity supply of different units during 8 days. . . . 33
4.14 State of charge for LRC storage. . . . 34
4.15 State of charge for pressurized vessel storage. . . . 35
4.16 State of charge for the cryogenic tanks storage. . . . 35
4.17 The effect of separate limitations on the system cost. . . . 37
4.18 The effect of separate limitations on the installed capacity of technology units in Case 1. . . . 37
4.19 The effect of double limitations on the system cost. . . . 39
4.20 The effect of double limitations on the installed capacity of technology units in Case 1. . . . 39
4.21 The effect of excluding one storage option on the system cost. . . . 40

4.22 The effect of the investment cost of the liquefaction plant on the system cost and liquefaction plant capacity. 41
4.23 The effect of the investment cost of the liquefaction plant on the capacity of LRC and cryogenic tank. 42
4.24 The effect of the daily boil off losses on the system cost and cryogenic tank capacity. 42

C.1 Load duration curve for electricity import for Case 1, 2 & 3. V
C.2 Load duration curve for electricity export for Case 1, 2 & 3. V
C.3 Load duration curve for hydrogen output from compressor 1 for Case 1, 2 & 3. VI
C.4 Load duration curve for hydrogen output from compressor 2 for Case 1 & 2. VI

D.1 The effect of single limitations on the installed capacity of technology units in Case 2. VII
D.2 The effect of single limitations on the installed capacity of technology units in Case 3. VII
D.3 The effect of single limitations on the installed capacity of the LRC and cryogenic tank in Case 1. VIII
D.4 The effect of single limitations on the installed capacity of the battery storage and pressurized vessel in Case 2. VIII
D.5 The effect of single limitations on the installed capacity of the LRC and cryogenic tank in Case 2. VIII
D.6 The effect of single limitations on the installed capacity of the battery storage and pressurized vessel in Case 2. IX
D.7 The effect of single limitations on the installed capacity of the LRC and cryogenic tank in Case 3. IX
D.8 The effect of double limitations on the installed capacity of technology units in Case 2. IX
D.11 The effect of double limitations on the installed capacity of the battery and pressurized vessel in Case 1. X
D.9 The effect of double limitations on the installed capacity of technology units in Case 3. X
D.10 The effect of double limitations on the installed capacity of the LRC and cryogenic tank in Case 1. X
D.12 The effect of double limitations on the installed capacity of the LRC and cryogenic tank in Case 2. XI
D.13 The effect of double limitations on the installed capacity of the battery and pressurized vessel in Case 2. XI
D.14 The effect of double limitations on the installed capacity of the LRC and cryogenic tank in Case 3. XI
D.15 The effect of double limitations on the installed capacity of the battery and pressurized vessel in Case 3. XII

E.1 The electricity consumption of the electrolyzer for 8 days in January. XIII
E.2 The electricity consumption of the liquefaction plant. XIII

E.3 The electricity consumption of compressor 1. XIV
E.4 The electricity consumption of compressor 2. XIV
E.5 The electricity consumption by the battery-electric aircraft. XIV
E.6 The electricity exported to the grid. XIV
E.7 The electricity supply from local wind turbines. XV
E.8 The electricity supplied from local solar PVs. XV
E.9 The electricity supplied from the grid. XV

List of Tables

3.1 The cases investigated in the thesis. 15
3.2 Units and descriptions of the profiles used throughout the thesis. . . . 16
3.3 Units and descriptions of variables used throughout the thesis. 16
3.4 Selected cost data from literature for technologies, storage and local generation of electricity. 22
3.5 Parameter data for technologies and local generation of electricity. . . 24
3.6 Parameter data from the literature for storage of hydrogen and electricity. 24
3.7 Densities for hydrogen for storage pressure and temperature [65]. . . 25

4.1 Annual amount of hydrogen demand for each case. 27
4.2 Annual amount of electricity and hydrogen demand for each case. . . 27
4.3 The time that the storage can supply the average hydrogen demand. . 34
4.4 Required area for the hydrogen and electricity units. 36
4.5 Required volume for the storage units. 36
4.6 Average marginal cost of electricity for aviation fuels. 36
4.7 Consumption based cost for aviation fuels. 36

A.1 Efficiencies for battery-electric [66] and JET-engine [67]. I

1

Introduction

Since the industrialization, the Earth's average temperature has increased by 1 °C, caused by the elevated emissions of greenhouse gases to the atmosphere, as a result of human activities [1]. The growing concerns about climate change have led to the Paris Agreement, an international contract urging to take action in order to decrease the pace of global warming. In the Paris Agreement, it is stated that the Earth's average temperature increase prior the industrial revolution should be limited to well below 2 °C [1]. However, by limiting the global warming to the more ambitious target of 1.5 °C shows a significant reduction of climate change effects [1].

To be able to fulfill the temperature targets, the carbon emissions need to be significantly reduced [1]. One considerable source of anthropogenic carbon emission comes from the aviation sector, which stands for 2-4% of the total global carbon emissions. Since aviation is expected to continue to grow by 3-5% per year, it places pressure on decarbonizing the aviation industry [2]. One of the companies that is facing this challenge is the Swedish state-owned company Swedavia AB, which has set goals to enable the transition toward fossil-free airports [3].

The Swedish company Swedavia AB owns and operates 10 of the airports in Sweden, whereof 4 ot them are international airports [3]. To be able to reduce the emissions, Swedavia AB has set up goals for the company to path the way for a transition to decarbonize the aviation industry. Two of the set goals are that all domestic flights should be fossil-free in 2030 and in 2045 all flights departing from an airport operated by Swedavia AB should be fossil-free. To be able to fulfill these goals, options like hydrogen, batteries and fossil-free jet fuels are part of the strategic plan [4]. In 2020 Swedavia AB became the first airport operator to be fossil-free in their own operation. Some of the measures taken were green electricity, hydrotreated vegetable oil (HVO) and biogas for vehicles and reserve power [5].

This paper will delve into the direct (battery-electric) and indirect electrification (hydrogen production) of Göteborg Landvetter Airport operated by Swedavia AB which is Sweden's second largest international airport. In 2023, Göteborg Landvetter Airport offered direct flights to 80 destinations and had around 5.2 million travelers [3]. During the climate conference COP28 in 2023, Göteborg Landvetter Airport was one of the first airports among 9 others, to receive level 5 of the Airport Carbon Accreditation (ACA) certification [6]. This indicates, among other things, that the airport has currently reduced their own greenhouse gas emissions with at least 90% and has a well-established plan to achieve reduction targets and reach net zero

emissions at latest 2050 [7].

There are multiple ways of decarbonizing the aviation sector, e.g. through the use of batteries, hydrogen fuel cells, combustion of hydrogen and sustainable aviation fuels (SAF) [8]. SAF is a broad term, which often is defined as a fuel which aims to replace the conventional jet fuel, kerosene, with synthetic fuels or biofuels. Synthetic fuels are generally produced from carbon dioxide and hydrogen while biofuels can be produced from a wide range of feedstocks such as forest- and agriculture residues, food waste, fats and oils [9]. SAF commonly refers to a drop-in fuel, that is so chemically similar to kerosene that it can replace up to 50% of conventional jet fuel without modifications to the engine [10]. This is the definition used when referring to SAF throughout this thesis. SAF is technically not limited by distance and can be used for a broad distance range. However, it is currently limited by its cost competitiveness to conventional jet fuel and biomass resources [11].

Battery-electric aviation has the benefits of no emissions during flight and high energy efficiency. However, it is limited in flight range due to a high weight-to-energy ratio of batteries [8]. To increase the flight range when electrifying the aviation industry, indirect electrification in form of hydrogen can be an option since it has the advantage of a high specific energy. Hydrogen can be produced through water electrolysis by applying electrical current. It can be used for aviation either via fuel cells or combustion of hydrogen [8]. In the case of hydrogen fuel cells, the hydrogen is converted to electricity which is used for driving the electric motor. This option has the potential of reducing the $CO_{2,eq}$ by 75-90% in relation to fossil jet fuel, where the remaining emissions are caused by water vapor and contrails [8]. Hydrogen can also be combusted in a turbine to generate propulsion, where the $CO_{2,eq}$ can be reduced by 50-75%. Hydrogen combustion has a higher climate impact than fuel cells due to the formation of NO_x as well as contrails [8]. Since hydrogen is applicable for a wide range of flight distances, it can potentially be one of the main technologies to decarbonize the aviation industry [8].

Swedavia's plan on decarbonizing the aviation industry with electrification, both directly by batteries and indirectly with hydrogen, will result in a large electricity demand. In this study, the case of Göteborg Landvetter Airport will be considered.

1.1 Aim

The aim of this thesis is to investigate how the electricity and hydrogen demand can be fulfilled at Göteborg Landvetter Airport by considering the option of onsite production and import of electricity and hydrogen. In both cases the liquefaction will take place onsite. The increased electricity demand will consider the water electrolysis, compressors, hydrogen liquefaction and the recharging of electric planes. More specifically, this thesis will investigate the following research questions:

- What is the expected demand of hydrogen and electricity in order to decarbonize the current aviation traffic departing from Göteborg Landvetter Airport?
- How can the predicted electricity and hydrogen demand be fulfilled?

1.2 Limitations

This project will consider the following limitations:

- For the onsite production, the project is limited to investigate hydrogen produced through electrolysis and will not investigate other production alternatives.
- Imported hydrogen should originate from Sweden only.
- It is assumed that the increased electricity demand at Göteborg Landvetter Airport will not affect the electricity prices in SE3.
- The liquefaction process will only be performed onsite.
- Hydrogen production to produce synthetic fuels will not be taken into account.
- Onsite is defined within the energy system that is to be modeled. The exact distance between the onsite technologies and airport will be determined by safety regulations which is outside the scope of this project.
- Potential risks of implementing the technologies near the airport are not investigated in this thesis.

2

Theory

The following chapter will present the theoretical background behind the electric and hydrogen powered aircraft as well as the technology units relevant for this project. Here including, water electrolysis (2.1.1), liquefaction (2.1.2), storage (2.1.3), compression (2.1.4) and import of hydrogen (2.1.5) as well as electricity storage and production (2.2).

2.1 Hydrogen for Aviation

Hydrogen has a low volumetric density and therefore needs to be compressed or liquefied in order to increase the density, where the highest energy per volume is obtained in liquid state [12]. In a study by Prewitz, Bardenhagen and Beck [12], it can be seen that a theoretical fuel tank with a volume of 20 m^3 could reach flight distances of approximately 1850 km with an on-board storage pressure of 700 bar. However, the challenge of integrating this volume on-board needs to be solved [12]. In a study by Mukhopadhaya [13], retrofit options of ATR 72 turboprop aircraft are investigated for both compressed hydrogen at 700 bar as well as liquid hydrogen. The results showed that ATR 72 could reach a flight range of approximately 1000 km. This is however reached with 42 passengers in comparison to the 78 passenger in the non retrofitted option of Jet A1 [13]. In the same study, the retrofit for liquid hydrogen reaches flight ranges of approximately 1750 km with 42 passengers [13]. According to the study by Smith and Mastorakos [14], liquid hydrogen can reach flight distances of up to 6000 km with 204 passengers by 2050 [14]. Another study preformed by Mukhopadhaya [15], estimates that liquid hydrogen will likely be cheaper than synthetic e-kerosene for routes up to 3400 km for passenger flights with up to 165 passengers.

2.1.1 Water Electrolysis

The majority of produced hydrogen in the world is currently being used in ammonia production, methanol production and oil refining [16]. About 95% of all hydrogen is generated through utilization of fossil fuels [17], primarily natural gas, coal and heavy oils [18]. The most common production method is steam methane reforming (SMR) which accounts for roughly 50% of all hydrogen production [19]. Other common production routes are partial oxidation of hydrocarbons, coal gasification [17] and hydrocarbon pyrolysis [18]. Hydrogen has also in recent years gained significant

attention for new applications. It has a high specific energy and it generates carbon free electricity through reaction with oxygen [18]. However, due to heavily increased anthropogenic greenhouse gas emissions which directly impact the environment and climate, new sustainable and non-carbon based production routes for hydrogen have to be implemented.

One of the most promising production alternatives for hydrogen is water electrolysis that utilizes renewable energy [16] which in the literature is frequently denoted as green hydrogen [20]. Water electrolysis is a process where the non-spontaneous formation of hydrogen from water is induced by applying electrical current [16]. Hydrogen is produced at the cathode and oxygen is produced at the anode. Between these two electrodes, there is always an electrolyte to enhance the flow of ions which is the main factor that sets apart different electrolyzer technologies [18].

Solid oxide electrolyzers (SOE) are still under development and successful scalability has yet to be proven [20]. The electrodes are made of pure nickel while the electrolyte is made of solid ceramic membrane where the ionic agents O^{2-} pass through [16]. The operating temperatures commonly vary between 900-1000 °C which is relatively high compared to other electrolyzer technologies. Higher operating temperatures yield higher conversion efficiency of up to 90% at a lower electricity input, but it also translates into a higher electrolyte degradation [16]. The cold start-up time was estimated to be 10 hours year 2020 and is predicted to reach 5 hours by year 2050 [21]. However, due to the high operating temperature range, SOE is assumed to be inapplicable for Göteborg Landvetter Airport.

Proton exchange membrane electrolyzer (PEM) is a more mature technology than SOE [20]. This technology produces hydrogen at lower temperatures ranging between 70-90 °C. The electrolyte consists of a membrane made of fluorosulfonic polymers where the ionic agents H^+ flow through. The catalysts used at the electrodes are platinum and iridium oxide [16]. This system has higher efficiency than alkaline electrolyzers because of higher reaction kinetics at the cathode due to acidic conditions. It is possible to produce pressurized hydrogen of 50 bar and higher, but it is currently considered challenging [21], [22]. Moreover, this system has expensive components [20] and a significant difficulty in scalability for larger applications [16]. The cold start-up time was estimated to be 30 seconds year 2020 and is predicted to reach 12 seconds by year 2050, which opens up the opportunity of offering ancillary services [21]. However, it is assumed that the airport will not offer ancillary services to the electricity grid, making PEM a less cost competitive choice.

Alkaline water electrolyzers (AE) is the most used electrolyzer technology in large industrial scale [20] and the only technology considered for hydrogen production in this thesis. The electrode materials constitute of nickel and cobalt oxides while the electrolyte solution is most often liquid potassium hydroxide [16]. The ionic agents are OH^- that flow through a ceramic oxide diaphragm installed between the anode and cathode [18]. The operating temperatures are in the range of 65 °C to 100 °C and the conversion efficiency is most commonly between 60% and 80%. In order to reach high hydrogen purity, gas separators, gas scrubbers and gas purifiers are required, thus increasing the system's required area [23]. The main drawback

with these electrolyzers is the potential corrosion that can arise at the electrodes due to the alkali conditions [16]. The alkaline electrolyzer can produce hydrogen at the same pressure as the operating pressure, where the operating pressure often is between 1 atm and 30 bar [21], [22]. The cold start-up time was estimated to be 80 minutes year 2020 and is predicted to be less than 30 minutes by year 2050 [21].

Generally, the water that will be sent into the electrolyzer must be ultrapure in order to prevent contamination of the cell that can arise due to water impurities [23]. Thus, the electrolyzer will be coupled with a water treatment plant as significantly large quantities of ultrapure water are required for the electrolysis process. Based on the mass ratio between water and hydrogen gas, 9 kg of ultrapure water will be needed for 1 kg of hydrogen gas to be produced. Depending on the water source, different treatment procedures will be implemented and therefore different volumes of extracted water are needed [23].

The amount of oxygen produced from the electrolysis is 8 kg_{O_2}/kg_{H_2}. The oxygen and excess heat produced by the electrolyzer can be utilized in various ways. Oxygen can be used in paper and pulp mills, steel industry, oxyfuel carbon capture technologies etc., while excess heat can be utilized for district heating [23].

2.1.2 Liquefaction

Hydrogen can be liquefied before application in aircraft in order to increase the density of the fuel. At normal conditions, which are defined as a temperature of 20 °C and absolute pressure of 1 atm, gaseous hydrogen has a density of 0.0899 kg/m^3 while liquid hydrogen has a density of 70.8 kg/m^3. This means that a tank with liquid hydrogen holds 787 times more hydrogen than an equally sized tank filled with gaseous hydrogen [20]. At ambient pressure, liquefaction of hydrogen occurs at -253 °C, which is in the cryogenic temperature range. One major drawback of hydrogen in liquid form is the boil-off losses that depend on the exothermic conversion process of ortho-hydrogen into para-hydrogen. Para- and ortho-hydrogen are the two spin isomers of molecular hydrogen [24]. In order to obtain a long-term storage of liquid hydrogen with minimal losses, the para-hydrogen concentration should be in the range of 95% and 98% after the liquefaction process. Higher content of para-hydrogen is achieved through a catalytic conversion [24].

The majority of the commercial liquefaction plants are based on the Claude cycle [25]. The gaseous hydrogen feed is first pressurized in a two compressor step in order to perform the process as efficiently as possible. The cycle then proceeds with pre-cooling where hydrogen is cooled down to 80 K in an isobaric heat exchanger using liquid nitrogen as cooling load. Thereafter, cryogenic cooling is carried out in a refrigeration system consisting of three heat exchangers where the temperature decreases below 30 K. Here, impurities are removed via adsorption and a catalytic conversion of ortho-hydrogen to para-hydrogen is performed. Finally, the onsite liquefaction process continues with an adiabatically isolated expansion where liquid hydrogen is obtained [25]. The expansion process is performed in two steps, the first step uses an istentropic expander and the second step utilizes two isenthalpic throttles. The isentropic expander helps the process to reach a higher temperature

reduction in comparison to only using isenthalpic throttles, thus increasing the cycle efficiency [25].

The energy consumption of the current liquefaction plants is in the range of 10-20 kWh_{el}/kg_{H_2} [26]. However, new research is aiming at reducing the energy consumption down to 6 kWh_{el}/kg_{H_2}. One of the most researched cycles is the mixed refrigerant cycle that has the advantage of a wider temperature range than a single refrigerant. Subsequently, the process can be supplied with cooling load over an extended temperature interval resulting in higher exergy efficiency [25].

The Argonne National Laboratory has developed a model where different hydrogen delivery scenarios are compared [27]. The Hydrogen Delivery Scenario Analysis Model (HDSAM) is frequently used in reports published by the Department of Energy (DOE) in USA. Moreover, HDSAM has derived a cost function for the capital cost of liquefiers by retrofitting the cost of different industrial liquefaction plants [26] and is presented in Appendix B. A function estimating the electric consumption of the liquefaction plants (ε_{Liq}) was obtained in a similar way and is presented in Equation 2.1. Here, Cap_{Liq} is the capacity of the liquefaction process and should be expressed in terms of tonnes per day (tpd).

$$\varepsilon_{Liq} = 13.382 \cdot Cap_{Liq}^{-0.1} \tag{2.1}$$

2.1.3 Hydrogen Storage

The following section will present different types of storage technologies relevant for this project for both liquid and gaseous hydrogen, more specifically Lined Rock Cavern (LRC), pressurized vessels and cryogenic tank.

Liquid Hydrogen Storage

Liquid hydrogen storage has the advantage of high energy density. Hydrogen has also a low boiling point, thus needing cryogenic environment for storage in liquid phase. Cryogenic hydrogen tanks are described to have double walls with a thermal insulation between the inner and outer wall which is obtained by applying vacuum [28]. This specific set-up minimizes heat losses and increases efficiency. However, boil-off losses will still occur (up to 5% per day) making vessel design an important aspect [25]. The main objective is to reduce the surface-to-volume ratio of liquid hydrogen which is obtained if spherical tanks are implemented [29]. Another disadvantage is the high energy penalty that comes with the liquefaction process described in Section 2.1.2. Linde PLC is one of the main manufacturers of cryogenic tanks for hydrogen storage. In 2019, they estimated that a container with a capacity of 3000 kg liquid hydrogen (approx. 42 m^3 or 100 MWh) had a filling time of 3 hours and off-loading time of 30 minutes [30]. The largest cryogenic tanks for storage of liquid hydrogen are owned by NASA's Kennedy Space Center in Florida [31]. In 1965, their first two cryogenic tanks were built in order to support the Apollo project and had a storage volume of 3400 m^3 each [31]. In 2018, a new tank began construction which will hold 4732 m^3 liquid hydrogen. The maximum boil-off losses are estimated to be 0.048% per day. On the other hand, HDSAM

predicts that the boil-off losses will decrease to 0.03% per day for large scale tanks in the future [27]. The HDSAM model also estimates the investment cost of the tank in terms of the tank volume, where 95% of the stored liquid hydrogen can be withdrawn. This equation can be found in Appendix B.

Gaseous Hydrogen Storage

Gaseous hydrogen storage includes both underground storage and compressed gas storage. Underground hydrogen storage can utilize geological features such as underground salt caverns and depleted gas or oil fields [32]. This type of storage has a low volumetric hydrogen density, low hydrogen losses and low investment costs per energy stored [25]. However, there are several limitations that arise due to the uneven global distribution of the caverns which moreover have to fulfill several requirements about capacity, physical conditions and environmental impact.

A special type of underground storage that has been proven to store natural gas is Lined Rock Cavern (LRC) with an existing facility in Skallen, southern Sweden. Solid rocks have a large availability across the globe, thus acting as an advantage when compared to salt caverns or depleted oil and gas fields [33]. This storage technology is still in the research stage for hydrogen, with one pilot plant currently being investigated for "green steel" production in Sweden. LRCs are created through mining solid rock and constructing two different layers, one consisting of concrete and the other of metal, typically steel. The concrete layer offers stability, prevents entrance of impurities from the surrounding rocks and preserves the rock from deteriorating. On the other hand, the inner steel liner prevents gas leakage and chemical reactions with hydrogen. The hard rock mass provides mechanical support for the gas tank filled with pressurized hydrogen [33]. This type of storage is however more expensive than salt caverns as it requires more construction and materials [34].

Lined rock caverns could be an option for large scale hydrogen storage for capacities in the size range of GWh to TWh with a discharge time ranging from days to weeks [35]. Based on the existing LRC in Skallen, the corresponding injection rate is 1300 kg/h (43 MWh/h) while the withdrawal rate is 3600 kg/h (120 MWh/h) for hydrogen [36]. The investment cost per unit of stored energy for the LRC is dependent on the maximum storage pressure, where it decreases with an increased pressure. According to Papadias [34], the capital investment cost goes from 3800 $€_{2024}$/MWh at 75 atm down to 1800 $€_{2024}$/MWh at 300 atm [34]. In LRC, the stored hydrogen is divided into cushion gas and working gas, where the cushion gas purpose is to maintain the pressure in the storage. The share of cushion gas increases with a higher maximum operating pressure in the LRC. However, as more hydrogen can be stored in the same volume, it results in decreased investment cost per energy [34].

Compressed gaseous hydrogen storage in cylindrical pressurized tanks that can be of four different types, are used for different applications and mainly for short term storage. Type I and II are the heaviest of all options due to their metal composition, thus most suitable for stationary applications. Type III and IV consist of composite materials and are therefore lighter making them more suitable for portable applications [28]. Another difference between the types is the operating

pressure. Type I tanks operate at pressures lower than 250 bar while Type II operate at a pressure of up to 800 bar, Type III up to 750 bar and Type IV up to 1000 bar [32]. The reason why Type IV tanks can withstand such a high pressure is due to the entire outer casing being made of carbon fiber [32], which is also the main cost driver of the storage unit [37]. The inner layer is made of a dense polymer liner preventing hydrogen from diffusing through the wall [32]. Type IV tanks are also considered to have the highest potential of commercialization and are predicted to break through in the automotive industry. DOE has already set a target of 60 kg H_2 regarding the storage capacity [38]. As a result, Type IV tanks are expected to have the highest cost reductions in the future [32].

2.1.4 Hydrogen Gas Compression

If hydrogen has to be transported or stored in gaseous form, it is generally compressed in order to increase the density and reduce the space it takes up [39]. Hydrogen compressors are divided into mechanical and non-mechanical compressors. The mechanical compressors include reciprocating compressors where the piston moves back and forth in the cylinder resulting in an increased pressure of the hydraulic fluid, thus compressing the gas. These type of compressors can reach high compression ratios due to the process being closer to isentropic conditions [39]. Reciprocating compressors can also provide flexibility since they can manage large flow variations [40]. Non-mechanical compressors include hydride and electrochemical compressors. The advantage of these compressors lies in their smaller size, no moving parts and lower noise [39].

Hydrogen compression involves multiple working stages, thus requiring inter-stage cooling in order to decrease the temperature which in turn reduces the compression work [40]. However, there are energy losses associated to the cooling operation and the shaft power which affect the compressor performance and the operational costs. Danish Energy Agency estimates in their report about "Transport of Energy" (2021) that the electric consumption of the hydrogen compressors (ε_{Comp}) for year 2050 can be calculated by using Equation 2.2. Here, P_{out} is the discharge pressure [bar] and P_{in} is the suction pressure [bar] of the compressor.

$$\varepsilon_{Comp} = 0.008 \cdot \left(P_{out}^{\frac{1}{3}} - P_{in}^{\frac{1}{3}} \right) \cdot \frac{1}{e^{H_2}} \tag{2.2}$$

One important challenge with hydrogen compression is lubrication because of reactions that can occur between hydrogen and hydrocarbons in mineral oil, thus resulting in oil contamination [41]. Since high purity hydrogen is generally required, dry compression is therefore the most suitable option making reciprocating compressors the most optimal choice for hydrogen compression [40].

2.1.5 Import of Hydrogen

Hydrogen can be transported in different ways depending on capacity, phase and distance. Liquid hydrogen can be transported with trucks and ships, while compressed hydrogen can be transported through pipeline and trucks [42]. Today,

pipelines are commonly used for transport of natural gas. However, as the demand for green hydrogen and the share of intermittent energy increases, pipelines gain more interest as an option for hydrogen transport [43]. Pipelines used for natural gas are not suited for hydrogen transport as hydrogen is a smaller and more reactive molecule making it harder to contain [44]. The cost of hydrogen transport via pipeline is dependent on the capacity of the pipeline, where the cost per transported hydrogen decreases for larger capacities [40]. The estimation by Danish Energy Agency for 2050 is 3.6 €/MW/m for capacities up to 100 MW and 0.2 €/MW/m for capacities above 6000 MW for a pipeline with a design pressure of 70 bar [45]. Pipelines have the advantage of low operating cost, high efficiency and low cost per transported hydrogen for large capacities. The main drawbacks are high investment cost and the difficulty for small scale implementation [42].

For hydrogen transport in small scale and short distances, trucks could be a suitable option. However, it is a less energy effective way of transport and has a higher variable operating cost due to driver labor and fuel consumption when compared to pipelines [42]. The unloading and loading time is expected to be 3 hours for compressed hydrogen in 2050, but it is currently 4.25 hours [40].

2.2 Electricity for Aviation

Through the use of batteries it is possible to reduce the energy losses from the aviation industry, due to their relatively high efficiency in comparison to other energy carriers. One of the barriers for batteries is the low capacity per mass, which limits the travel range and weight of aircraft and thereby the amount of passengers. Another practical issue is that battery-electric aircraft have a lower flight speed in comparison to conventional aircraft, and thereby could cause disturbances in the flight schedule [46]. The battery capacity also needs to be large enough to have reserve capacity, if landing is hindered. This means that the available capacity for the battery which can be allocated to travel distance is lower than the actual battery capacity. In a study by Mukhopadhaya [47], where the estimated energy density of the battery for 2050 is 500 Wh/kg, the cruise range could reach between 650 km up to 1100 km depending on the allowed mass of the battery. This does however not include reserve capacity. Moreover, the operational cruise range was between 280 km up to 500 km depending on aircraft configuration [47].

2.2.1 Lithium Batteries

One widely used electric energy carrier is the lithium-ion battery which consists of two electrodes. The cathode is commonly made of graphite and the anode often made of a metal oxide. The electrolytic solution consists of a lithium salt dissolved in an organic solvent [48]. The electrodes are separated by a porous membrane, thus hindering contact between the anode and cathode and thereby avoiding short-circuiting [32]. The porosity of the membrane allows the lithium ions to pass through. If the temperature rises too high, the membrane starts melting and thus blocking the passage of the ions [48]. When lithium batteries are being charged, the

lithium ions move from the cathode to the anode induced by an electric current while discharge occurs when the ions are moving back to the cathode. The losses from the battery can be divided into standby losses as well as losses that occur during charge and discharge which are caused by resistance and conversion from chemically stored energy to electricity [32].

Apart from being used in airplanes, lithium-ion batteries can be used for load shifting and peak reduction in an energy system due to the characteristics of fast charge and discharge rate. They can also be used to provide ancillary services such as frequency and voltage regulation as well as electricity storage. The implementation of batteries in the grid can therefore be used to increase the integration of intermittent electricity generation [32]. Batteries are expected to grow in road transportation market as well as portable electronics and energy storage applications [48].

2.2.2 Wind and Solar Power in the Airport Environment

Production of renewable electricity via wind turbines and solar PVs is of greatest interest in this thesis due to the requirement of green hydrogen, the fulfilling of climate goals and the possibility for implementation close to the airport (when compared to e.g. nuclear power).

There are however several safety concerns and regulations related to the implementation of wind turbines close to the airport regarding height, noise levels and electromagnetic radiation. In the context of airports within EU, there are certain height limitations within a specific radius from the centre of the airport. Generally, the restricted area has a radius of 15 km. Firstly, a 45 meters height limitation comes into effect and applies over an elliptical shaped area with a radius of 4 km from each of the strip-ends of the runway [49]. This area is called the inner horizontal surface. Thereafter, the height limitation steadily increases following a conical shape, thus creating another horizontal area that is typically referred to as the conical surface. Then, a 150 meters height limitation applies over the remaining area which is called the outer horizontal surface [49]. Moreover, there are additional restrictions within the inner horizontal and conical surfaces that aim at protecting the aircraft during approach, landing, take-off and climbing. Wind turbines result also in radar interference due to reflection of electromagnetic radiation [50].

The safety concerns regarding solar PVs for local electricity production include reflection, radar interference and the presence of an object near the runway. There is a fear that solar PVs will reflect light and will cause lower visibility or flash blindness for airport operators and pilots, thus creating a safety hazard [51]. However, it is uncertainties related to the reflectivity of solar PVs due to lack of data which results in the use of the maximum solar irradiation when examining the implementation of solar PVs close to the airport. This results in an overestimation of the light reflection from the solar PVs, as in reality, most PVs have anti-reflection coating designed to reduce reflection [51]. Another safety concern is that the metals in the PV can interfere with radar signals and thus cause disturbances for the air traffic [51]. Lastly, the required area for the installation of the solar PVs is generally large due to the low power output per unit area.

3

Methods

The method used to assess the aim of this thesis was divided into four parts. The first part of the project consisted of literature research. The second part consisted of data collection, including flight distances and departure times, in order to map the flights departing from Göteborg Landvetter Airport. The mapping of flights was performed in Excel by categorising them into different flight ranges. These ranges were later converted to hydrogen and electricity demand profiles with an hourly time resolution. The third part included the set up of the objective function with the constraints that the hydrogen demand and recharging of electric airplanes from the hourly profiles need to be fulfilled. The models objective function was the total system cost including fixed and variable operating costs as well as annualized investments. The optimization model was developed in GAMS. The fourth part of the project was analysis of the output data from the different scenarios and sensitivity analysis of certain parameters in order to determine the robustness of the obtained results.

The following sections will go through the method into further details, more specifically about the construction of the demand profiles (3.1), the development of the optimization model (3.2), the selected parameter data from the literature (3.3) and the performed sensitivity analysis (3.4).

3.1 Construction of Demand Profiles

The entire electricity and hydrogen demand for the airplanes departing from Göteborg Landvetter Airport are assumed to be covered by the airport itself. This was done in order to account for the energy demand required for the entire flight distance. All flights departing within one hour were aggregated and converted to energy demand by using the current amount of jet fuel consumption as shown in Equation 3.1. This particular calculation was repeated for all hours of the year, thus laying the foundation for the hourly energy demand profiles.

$$E\,[\text{MWh}] = d\ [\text{km}] \cdot JC \left[\frac{\text{liter}}{\text{km}}\right] \cdot \rho \left[\frac{\text{kg}}{\text{liter}}\right] \cdot e^{Jet} \left[\frac{\text{MJ}}{\text{kg}}\right] \cdot \frac{1}{3600} \left[\frac{\text{MWh}}{\text{MJ}}\right] \tag{3.1}$$

Here, E is the total energy demand for each hour, d is the flight distance, JC is the jet fuel consumption, ρ is the density of Jet A-1 and e_{Jet} is the specific energy content of Jet A-1. The conversion to electricity and hydrogen demand was done by

using Equations 3.2, 3.3 and 3.4. Note that Equations 3.3 and 3.4 assume the same efficiency for hydrogen utilization in aircraft as for combustion of jet fuel.

$$D_t^{BEA} = E_{BatteryRange} \cdot \frac{\eta_{JetEngine}}{\eta_{EM} \cdot \eta_{Electronics} \cdot \eta_{Dist} \cdot \eta_{Management}} \tag{3.2}$$

$$D_t^{H_2} = E_{H_2Range} \tag{3.3}$$

$$D_t^{LH_2} = E_{LH_2Range} \tag{3.4}$$

Here, D_t^{BEA} is the hourly energy demand for charging of battery-electric aircraft, $D_t^{H_2}$ is the hourly energy demand for refueling of hydrogen gas powered aircraft and $D_t^{LH_2}$ is the hourly energy demand for refueling of liquid hydrogen powered aircraft. Moreover, η_{EM} is the efficiency of electrical motor, $\eta_{Electronics}$ is the efficiency of power electronics, η_{Dist} is the distribution efficiency and $\eta_{Management}$ is the efficiency of energy management. See Table A.1 in Appendix A to find the efficiency values used for this thesis. In the cases where flexible charging is applied to airplanes standing over the night that depart before 8 a.m., the load can be supplied between 0 a.m. to the hour before departure. Thereby, the electricity load from the battery-electric aircraft (BEA) was divided as a flexible load $D_t^{BEA,Flex}$ and a fixed load $D_t^{BEA,Fixed}$ as shown in Equation 3.5.

$$D_t^{BEA} = D_t^{BEA,Flex} + D_t^{BEA,Fixed} \tag{3.5}$$

When all the hourly energy demand profiles were constructed, a set t of timesteps containing all the hours of the year, a set A containing technologies and a set B containing storage units were created. All elements of the sets are listed below.

$$\begin{aligned} t \in T =& \{1, 2, ...8760\} \\ \alpha \in A =& \{\text{wind power, solar PV, cable, electrolyzer, liquefaction} \\ & \text{pipeline, trucks, compressor 1, compressor 2}\} \\ \beta \in B =& \{\text{battery, LRC, } H_2\text{-Tank, } LH_2\text{-Tank}\} \end{aligned}$$

Thereafter, the objective function was formulated including annual investments as well as fixed and variable costs. Then, the supply demand balance of electricity was set up followed by all the constraints for the technology units.

3.1.1 Cases

Based on the presented data from the literature and discussion with Swedavia, five different flight distance ranges were chosen to be investigated. Battery-electric aircraft was investigated for flight distances of up to 400 km. This technology was discarded for the remaining cases where only hydrogen powered aircraft was investigated for all distances up to 3100 km. Flight distances above 3100 km were assumed to be covered by SAF and were therefore not taken into consideration in this project. For each scenario, both hydrogen import via pipeline and trucks, and onsite production via the electrolyzer were studied in combination with each other. A summary of the three cases is presented in Table 3.1.

Table 3.1: The cases investigated in the thesis.

	$\leq$ 400 km	400-800 km	800-1500 km	1500-3100 km
Case 1	Electricity	H_2	H_2	LH_2
Case 2	H_2	H_2	LH_2	LH_2
Case 3	LH_2	LH_2	LH_2	LH_2

3.2 Energy System Model

The investigated energy system is presented in Figure 3.1 where the green lines describe the path of the electricity, the blue lines describe the gaseous hydrogen flow and the red lines describe the liquid hydrogen flow. The bars labeled with A, B, C, D, E, F, G and H represent the points where energy balances are set up. The energy system includes an alkaline electrolyzer, liquefaction plant, compressors, electricity generation technologies, a cable connection to the electricity grid, battery storage and hydrogen storage in LRC, cryogenic tank and pressurized vessels.

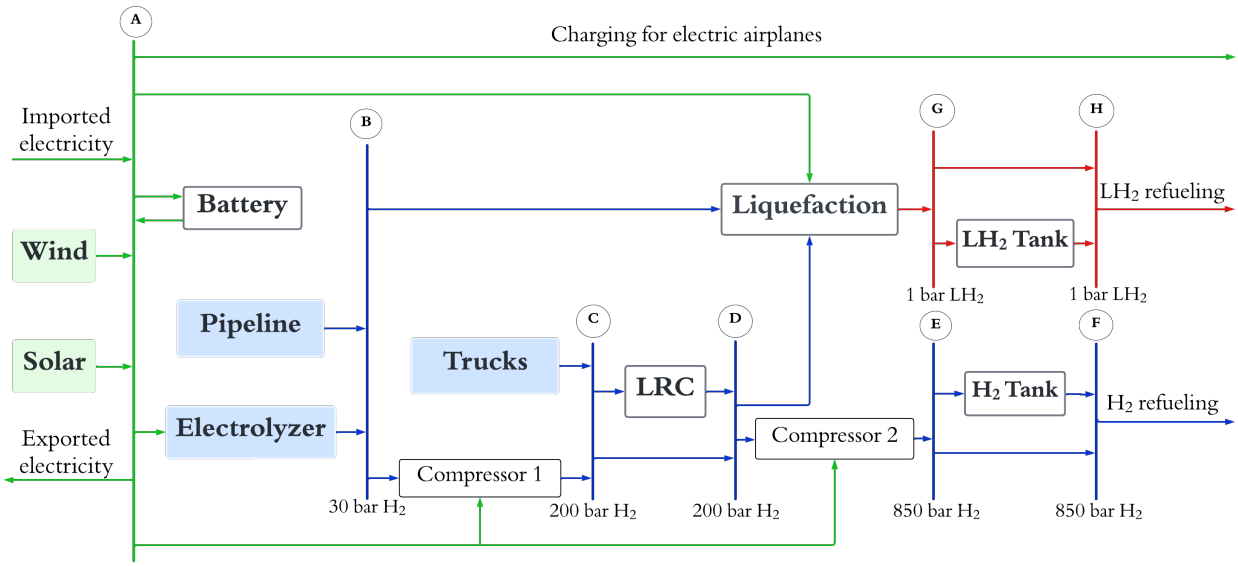

Figure 3.1: A visual representation of the energy system including electricity and hydrogen flows, where LH_2 is liquid hydrogen and H_2 is gaseous hydrogen.

The alkaline electrolyzer was chosen as the only hydrogen production unit as it is a mature and well proven technology. Battery storage was implemented in order to support and stabilize the system. LRC was implemented in order to store large volumes of hydrogen and thus utilize periods of high electricity supply. The cryogenic tank and the pressurized vessels were chosen in order to increase the flexibility of the system by storing hydrogen in the same temperature and pressure range as the demand requires. The pressurized vessel storage was chosen to be a type IV tank operating at 850 bar. The hydrogen containers in the airplanes were assumed to

operate at 700 bar so the pressure vessel storage onsite was modeled to operate at a higher pressure in order to obtain a pressure difference acting as a driving force for the fluid flow. Two transportation methods for import of hydrogen were also studied which include pipeline and trucks. Moreover, the model was always allowed to invest in local electricity production consisting of wind and solar power. All the variables and profiles used throughout the thesis are presented in Table 3.2 and 3.3.

Table 3.2: Units and descriptions of the profiles used throughout the thesis.

Profiles	**Unit**	**Description**
D_t^{BEA}	[MWh_{el}/h]	Total electricity demand for charging of BEA
$D_t^{BEA,Fix}$	[MWh_{el}/h]	Fixed electricity demand for charging of BEA
$D_t^{BEA,Flex}$	[MWh_{el}/h]	Flexible electricity demand for charging of BEA
$D_t^{H_2}$	[MWh_{H_2}/h]	Refueling demand of gaseous hydrogen
$D_t^{LH_2}$	[MWh_{LH_2}/h]	Refueling demand of liquid hydrogen
C_t^{el}	[€$_{2024}$/MWh]	Electricity price
$CF_{g,t}$	[-]	Capacity factor of electricity generation technologies

Table 3.3: Units and descriptions of variables used throughout the thesis.

Variable	**Unit**	**Description**
X_t^{el}	[MWh_{el}/h]	Export of electricity
$P_{\alpha,t}$	[MWh/h]	Produced electricity or hydrogen from technologies
F_t^{BtoLiq}	[MWh_{H_2}/h]	Feed hydrogen from point B to liquefaction
F_t^{DtoLiq}	[MWh_{H_2}/h]	Feed hydrogen from point D to liquefaction
F_t^{CtoD}	[MWh_{H_2}/h]	Hydrogen from point C to D (bypassing LRC)
F_t^{EtoF}	[MWh_{H_2}/h]	Hydrogen from point E to F (bypassing H_2 tank)
F_t^{GtoH}	[MWh_{H_2}/h]	Hydrogen from point G to H (bypassing LH_2 tank)
$F_t^{Recirculation}$	[MWh_{H_2}/h]	Recirculated boil-off losses sent for liquefaction
Cap_α	[MW]	Capacity of technologies
Cap_β	[MWh]	Capacity of storage
$SOC_{\beta,t}$	[MWh]	State of charge for storage
$Ch_{\beta,t}$	[MWh/h]	Charge of storage
$Disch_{\beta,t}$	[MWh/h]	Discharge of storage
$FlexCh_t$	[MWh/h]	Charge of flexible load from BEA

3.2.1 Objective Function

The total system cost is presented in Equation 3.6 where the objective function is minimized. The total system cost consists of capital expenditures (C^{CAPEX}), fixed operating costs (C^{FOM}) and variable costs (C^{VOM}) as well as cost of electricity (C_t^{el}) and hydrogen ($C^{\mathrm{H_2}}$). The capital expenditures were annualized with a discount rate of 5% according to Equation 3.7 and with the lifetimes presented in Table 3.5 and Table 3.6. The investment and fixed costs for technologies were based on the installed capacity. The investment costs for storage units were based on the maximum energy stored while the fixed costs were based on the maximum discharge rate. The variable costs were based on the total energy output from technologies and storage units during one year. The model was solved with a Linear Programming (LP) solver where the objective function was minimized for all the investigated cases. If the cost optimal solution included import of hydrogen, the cases were ran again with a Mixed Integer Programming (MIP) solver in order to activate the semi-continuous variables regarding pipeline for a more accurate and realistic solution.

The used electricity price (C_t^{el}) was taken from a model that studied the European future electricity system with net-zero carbon dioxide emissions year 2050 and was based on weather data from 2019 [52]. Therefore, the capacity factors profiles for Göteborg Landvetter Airport were taken for the same year (2019) [53]–[55]. The cost for hydrogen $C^{\mathrm{H_2}}$ was assumed to be constant over the year, and was taken as 110 €$_{2020}$/MWh [56].

$$\begin{aligned} C_{Sys} = & \sum_{\alpha \in A} Cap_\alpha \cdot (C_\alpha^{FOM} + C_\alpha^{CAPEX} \cdot a_\alpha) + \sum_{t \in T} \sum_{\alpha \in A} P_{\alpha,t} \cdot C_\alpha^{VOM} \\ & + \sum_{\beta \in B} Cap_\beta \cdot (C_\beta^{FOM} \cdot \gamma_\beta^{disch} + C_\beta^{CAPEX} \cdot a_\beta) + \sum_{\mathrm{t} \in T} \sum_{\beta \in B} Disch_{\beta,t} \cdot C_\beta^{VOM} \\ & + \sum_{t \in T} P_{Cable} \cdot C_t^{el} + \sum_{t \in T} (P_{Pipeline,t} + P_{Trucks,t}) \cdot C^{H_2} - X_t^{el} \cdot C_t^{el} + C_{Liq}^{TOT} \end{aligned} \tag{3.6}$$

Here a is the annuity factor that was calculated using Equation 3.7.

$$a = \frac{r}{(1 - (1 + r))^{-Lifetime}} \tag{3.7}$$

3.2.2 Electricity Balances

The electricity supply origins from electricity import from the grid ($P_{Cable,t}$) and onsite generation from wind power and solar PV ($P_{G,t}$) as well as the electricity discharged from the battery ($Disch_{Bat,t}$) according to Equation 3.8. Here, η_{Bat}^{disch} is the discharging efficiency of the battery storage.

$$Supply_t = P_{Cable,t} + \sum_G P_{G,t} + \eta_{Bat}^{disch} \cdot Disch_{Bat,t} \tag{3.8}$$

The electricity demand for each timestep is built up by the electricity consumption of the battery-electric aircraft, consisting of the flexible load ($FlexCh_t$) and the

fixed load (D_t^{BEA}), as well as the electricity supplied to charge the battery storage ($Ch_{Bat,t}$) and operate the energy-consuming technologies as shown in Equation 3.9. Here, $P_{Elec,t}$, $P_{Liq,t}$, $P_{Comp1,t}$ and $P_{Comp1,t}$ are the hydrogen outputs from the electrolyzer, liquefaction plant, compressor 1 and compressor 2 respectively while ε is the electricity consumption of each technology in terms of $\mathrm{MWh_{el}/MWh_{H_2}}$.

$$\begin{aligned} Demand_t = D_t^{BEA} + Ch_{Bat,t} + \varepsilon_{Elec} \cdot P_{Elec,t} + \varepsilon_{Liq} \cdot P_{Liq,t} \\ + FlexCh_t^{tot} + \varepsilon_{Comp1} \cdot P_{Comp1,t} + \varepsilon_{Comp2} \cdot P_{Comp2,t} \end{aligned} \tag{3.9}$$

The supply needs to be greater or equal to the demand for each timestep t according to Equation 3.10. This supply and demand balance of electricity is represented by point A in Figure 3.1.

$$Supply_t \geq Demand_t \tag{3.10}$$

The electricity generated by wind power and solar PVs was calculated by using Equation 3.11 where the capacity factor for each hour of year 2019 at Göteborg Landvetter Airport was multiplied by the installed capacity of wind power and solar PVs. The electricity generation was not allowed to exceed the available production determined by the installed capacity (Cap_g) and the capacity factor ($CF_{g,t}$).

$$P_{g,t} = CF_{g,t} \cdot Cap_g \tag{3.11}$$

The same constraint is set for the amount of exported electricity (X_t^{el}) in Equation 3.12 in order to not exceed the capacity of the power cable (Cap_{Cable}) between Göteborg Landvetter Airport and Härryda municipality.

$$X_t^{el} \leq Cap_{Cable} \tag{3.12}$$

3.2.2.1 Flexible Charging

For Case 1, the electricity demand between 5 and 8 a.m., is set to be flexible for all days of the year, which is noted as the hours h, which contains the hours (6, 7, 8). Thus, the electricity demand required for the battery-electric aviation is divided into a flexible part ($D_t^{BEA,Flex,h}$) for the airplanes standing over night and a fixed part ($D_t^{BEA,Fixed}$). The amount of electricity charged during night must be greater or equal to the electricity demand of the departing aircraft in the morning, as shown in Equation 3.13, where the demand at latest needs to be fulfilled when the demand occurs in the profile ($D_t^{BEA,Flex,h}$). This was implemented to ensure that the airplanes could charge up until the load actually needed to be fulfilled and thereby maximizing the allowed charging window.

$$ChNight_t^h \geq D_t^{BEA,Flex,h} \text{ for } h \in \{6, 7, 8\} \tag{3.13}$$

The charging was allowed to take place when the availability factor $n_t^a = 1$ which represented airplanes standing over night and available for charging from 0 a.m. until plane departure, as shown in Equation 3.14. Otherwise, the availability factor was $n_t^a = 0$ as the airplane either has departed or not yet arrived. To ensure that the airplanes were only charged during night until the following morning, the profile

n_t^r was used which consisted of ones during all hours of the year, except the hours corresponding to 1 p.m. each day.

$$ChNight_t^h = FlexCh_t^h \cdot n_t^a + ChNight_{t-1}^h \cdot n_t^r \text{ for } h \in \{6, 7, 8\} \tag{3.14}$$

The electricity supplied to the aircraft during nighttime corresponded to $FlexCh_t^{tot}$ as shown in Equation 3.15.

$$FlexCh_t^{tot} = FlexCh_t^6 + FlexCh_t^7 + FlexCh_t^8 \tag{3.15}$$

3.2.3 Hydrogen Balances

The hydrogen balances in this section are mainly based on the different pressure levels and points A-H presented in Figure 3.1. Hydrogen gas was introduced into the system through two different routes. The first route included onsite generation via the electrolyzer operating at 30 bar. The second route included import of hydrogen from the Port of Gothenburg where pipelines and trucks were options for transportation to Göteborg Landvetter Airport. Hydrogen transported via pipeline was assumed to have a pressure of 30 bar while hydrogen transported via trucks was assumed to have a pressure of 200 bar. These two streams were therefore introduced into the system at different stages. The hydrogen gas streams from the electrolyzer ($P_{Electrolyzer,t}$) and pipeline ($P_{Pipeline,t}$) were either sent to a compression step ($P_{Comp1,t}$) or the liquefaction plant (F_t^{BtoLiq}) as shown in Equation 3.16. In Figure 3.1, this balance is represented by point B. Hydrogen losses over the compressors were neglected and therefore, the hydrogen input was set equal to the hydrogen output.

$$P_{Electrolyzer,t} + P_{Pipeline,t} = P_{Comp1,t} + F_t^{BtoLiq} \tag{3.16}$$

The investment cost of pipelines is dependent on the capacity, thus the model was allowed to choose between different alternatives by using semi-continuous variables. In Equation 3.17, $P_{Pipeline100MW,t}$ corresponds to a pipeline with a capacity between 0 and 100 MW, $P_{Pipeline250MW,t}$ corresponds to a capacity between 100 and 250 MW while $P_{Pipeline500MW,t}$ corresponds to a capacity between 250 and 500 MW.

$$P_{Pipeline,t} = P_{Pipeline100MW,t} + P_{Pipeline250MW,t} + P_{Pipeline500MW,t} \tag{3.17}$$

The hydrogen going out from the first compression step had a pressure of 200 bar which also was the pressure of the imported hydrogen being transported via trucks. These two hydrogen streams could either be sent for storage in LRC ($Ch_{LRC,t}$) or to a second compression step (F_t^{CtoD}) as shown in Equation 3.18, which in Figure 3.1 is described by point C. Here, $Ch_{LRC,t}$ includes also the losses that occur during the charging of the LRC storage.

$$P_{Comp1,t} + P_{Trucks,t} \geq Ch_{LRC,t} + F_t^{CtoD} \tag{3.18}$$

The next balance shown in Equation 3.19 sets the discharge of hydrogen from the LRC storage ($Disch_{LRC,t}$) and the direct stream from compressor 1 (F_t^{CtoD}) equal

to the second hydrogen stream going in to the liquefaction plant (F_t^{DtoLiq}) and the hydrogen going in to compressor 2 ($P_{Comp2,t}$). This balance is represented by point D in Figure 3.1.

$$Disch_{LRC,t} + F_t^{CtoD} = F_t^{DtoLiq} + P_{Comp2,t} \tag{3.19}$$

The gaseous hydrogen coming out of compressor 2 was set equal to the input of the pressure vessel storage ($Ch_{H_2Tank,t}$) and the amount of hydrogen sent directly for refueling of airplanes (F^{EtoF}) which is described by Equation 3.20. In another hydrogen balance, the output from the liquefaction plant ($P_{Liq,t}$) was set equal to the charge of the cryogenic tank ($Ch_{LH_2Tank,t}$) and the amount of liquid hydrogen sent directly to the refueling station (F^{GtoH}), as shown in Equation 3.21. The cryogenic tank was assumed to operate at the same pressure as the liquefaction plant. Equations 3.20 and 3.21 can be visualised by point E and G in Figure 3.1.

$$P_{Comp2,t} = Ch_{H_2Tank,t} + F^{EtoF} \tag{3.20}$$

$$P_{Liq,t} = Ch_{LH_2Tank,t} + F^{GtoH} \tag{3.21}$$

The hydrogen energy balances shown in Equation 3.22 and 3.23 describe the demand profiles of gaseous hydrogen and liquid hydrogen by setting these profiles to being equal to or less than the amount of hydrogen sent directly for refueling and the output from each tank storage ($Disch_{H_2Tank,t}$ and $Disch_{LH_2Tank,t}$). These balances can be visualised by point F and H in Figure 3.1.

$$D_t^{H_2} \leq \eta_{H_2Tank}^{disch} \cdot Disch_{H_2Tank,t} + F_t^{EtoF} \tag{3.22}$$

$$D_t^{LH_2} \leq \eta_{LH_2Tank}^{disch} \cdot Disch_{LH_2Tank,t} + F_t^{GtoH} \tag{3.23}$$

Additionally, the capacity of each technology consisting of the electrolyzer, liquefaction plant, pipeline, compressors, cable, wind power and solar PVs, denoted as Cap_α, has to be greater or equal to the hydrogen or electricity output from each of the technologies respectively which is described in Equation 3.24.

$$Cap_\alpha \geq P_{\alpha,t} \tag{3.24}$$

For the liquefaction plant, hydrogen losses were also taken into account as shown in Equation 3.25 where $\eta_{Liq}^{losses} = 0.995$ [27]. Here, $F_t^{Recirculation}$ is the recirculated flow of the boil-off losses that emerge during storage and charging of the cryogenic tank, as shown in Equation 3.26.

$$\left[F_t^{BtoLiq} + F_t^{DtoLiq} + F_t^{Recirculation}\right] \cdot \eta_{Liq}^{losses} \geq P_{Liq,t} \tag{3.25}$$

$$F_t^{Recirculation} = (1 - \eta_{LH_2Tank}^{ch}) \cdot Ch_{LH2_Tank,t} + \delta_{LH_2Tank} \cdot SOC_{LH2_Tank,t} \tag{3.26}$$

The amount of energy in a storage for time step $t+1$ ($SOC_{\beta,t+1}$) is determined from the difference between the energy charged ($Ch_{\beta,t}$) and discharged ($Disch_{\beta,t}$) as well as the state of charge ($SOC_{\beta,t}$) and losses during storage at the current time step t. Here, δ_β is a fraction of hydrogen stand-by losses from storage and η_β^{ch} is

the charging efficiency of each storage. The state of charge is described in Equation 3.27, where the last timestep is equal to the first timestep of the year.

$$SOC_{\beta,t+1} = \eta_{\beta}^{ch} \cdot Ch_{\beta,t} - Disch_{\beta,t} - \delta_{\beta} \cdot SOC_{\beta,t} + SOC_{\beta,t} \tag{3.27}$$

The maximum charge ($Ch_{\beta,t}^{\max}$) and discharge ($Disch_{\beta,t}^{\max}$) are described in Equation 3.28 and 3.29. Here, the maximum charge and discharge rate is a function of the installed storage capacity. The charge/discharge is limited by the parameter γ which is the fraction of the storage capacity that can be charged/discharged during one timestep.

$$Ch_{\beta,t}^{\max} \leq \gamma_{\beta}^{ch} \cdot Cap_{\beta} \tag{3.28}$$

$$Disch_{\beta,t}^{\max} \leq \gamma_{\beta}^{disch} \cdot Cap_{\beta} \tag{3.29}$$

Moreover, the state of charge of each storage is limited by the maximum installed storage capacity (Cap_{β}), as shown in Equation 3.30.

$$SOC_{\beta,t} \leq Cap_{\beta} \tag{3.30}$$

3.3 Quantitative Data

In the following sections, data for each of the parameters used throughout the project will be presented along with a brief motivation to the selected parameter data. The parameters were divided into cost and technical parameters.

3.3.1 Cost Parameters

A large amount of the parameter data was taken from Danish Energy Agency [23]. The electrolyzer data was taken for a unit with a capacity of 100 MW of input electricity. This data was originally given in terms of electricity, but was later converted and expressed in terms of output hydrogen as shown in Table 3.4. The investment and fixed operational cost for the hydrogen pipeline was taken for three different capacities at an operating pressure of 70 bar. The model then chose the most cost optimal capacity while still fulfilling all the constraints. The direct distance between Göteborg Landvetter Airport and Port of Gothenburg was estimated to be 21 km. Cost data for pressurized H_2 Tank was taken for a type IV tank that can operate between 350 bar up to 1000 bar. Fixed costs were taken for type I since data could not be found for type IV. Moreover, for all storage alternatives, the fixed costs are given in terms of Euro per maximum discharged energy.

Table 3.4: Selected cost data from literature for technologies, storage and local generation of electricity.

Technologies	C^{CAPEX} $\left[\frac{\text{k€}}{\text{MW}_{\text{H}_2}}\right]$	C^{VOM} $\left[\frac{€}{\text{MWh}_{\text{H}_2}}\right]$	C^{FOM} $\left[\frac{€}{\text{MW}_{\text{H}_2}}\right]$
Electrolyzer [57], [58]	390	1.0	7800
Liquefaction* [27]	-	-	-
Pipeline 0-100 MW [45]	76	-	4.9
Pipeline 100-250 MW [45]	33	-	4.9
Pipeline 250-500 MW [45]	22	-	4.9
Truck Service [45]	-	5.4	-
Compressor 1 [59]	63	-	1900
Compressor 2 [59]	84	-	2500
Cable [60]	-	5.0	49000
Storage	C^{CAPEX} $\left[\frac{\text{k€}}{\text{MWh}_{\text{H}_2}}\right]$	C^{VOM} $\left[\frac{€}{\text{MWh}}\right]$	C^{FOM} $\left[\frac{€}{\text{MWh}_{\text{H}_2}}\right]$
H_2 Tank [23]	55	-	520
LH_2 Tank* [27]	1400	-	21
Battery [61]	330	2.1	702
LRC [34]	1.8	-	5900
Generation	C^{CAPEX} $\left[\frac{\text{k€}}{\text{MWh}_{\text{el}}}\right]$	C^{VOM} $\left[\frac{€}{\text{MWh}_{\text{el}}}\right]$	C^{FOM} $\left[\frac{\text{k€}}{\text{MW}_{\text{el}}}\right]$
Wind power [62]	1200	1.5	14
Solar PV [62]	340	-	8.7

*Cost for liquefaction and LH_2 tank were calculated by using Equation 3.32-3.35.

The capital investment cost for each compressor (C_{Comp}^{CAPEX}) was calculated by using Equation 3.31 [59] and was obtained in terms of €$_{2024}$/MWh. This equation is corrected to account for the inflation rate and currency conversion, yielding the value given in Table 3.4.

$$C_{Comp}^{CAPEX} = 2900000 \cdot \varepsilon_{Comp} \tag{3.31}$$

The variable cost of the installed cable is the so called grid-fee that accounts for the transmission losses. The fixed cost is based on the maximum power which the consumer is allowed to utilize during one year, thus covering the investment made by the owner of the grid. The hourly electricity price used in the calculations is modeled for 2050, but based on weather data from 2019 [52], and is presented below in Figure 3.2. The highest peak occurs in January between the timesteps 535-621 where the electricity cost is between 317-1914 €/MWh.

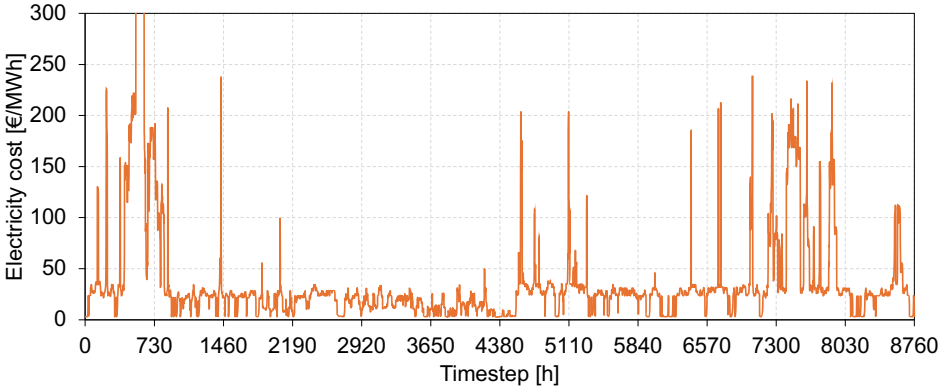

Figure 3.2: The hourly price profile of electricity for year 2050 based on weather data from 2019.

The yearly total cost of the liquefaction process (C_{Liq}^{TOT}) was based on HDSAM [27], and was calculated according to Equation 3.32 where it was obtained in terms of €/year. Here, C_{Liq}^{CAPEX} is the capital investment cost and C_{Liq}^{FOM} is the fixed cost. Detailed calculations of these costs are presented in Appendix B. Fixed costs (C_{Liq}^{FOM}) added up to 3.1% of the capital investment costs, see Equation 3.33.

$$C_{Liq}^{TOT} = C_{Liq}^{CAPEX} \cdot a_{Liq} + C_{Liq}^{FOM} \tag{3.32}$$

$$C_{Liq}^{FOM} = 0.031 \cdot C_{Liq}^{CAPEX} \tag{3.33}$$

The total capital investment cost ($C_{LH_2Tank}^{CAPEX}$) was calculated as shown in Equation 3.34 and was obtained in terms of $€_{2024}$. Here, $C^{Equipment}$ is the equipment cost, C^{Other} is other capital costs and C^{BOP} is balance of plant costs. Detailed calculations of these costs are presented in Appendix B. The total fixed costs ($C_{LH_2Tank}^{FOM}$) added up to the same ratio of the capital investment cost for the liquefier, as shown in Equation 3.35.

$$C_{LH_2Tank}^{CAPEX} = C^{Equipment} + C^{Other} + C^{BOP} \tag{3.34}$$

$$C_{LH_2Tank}^{FOM} = 0.031 \cdot C_{LH_2Tank}^{CAPEX} \tag{3.35}$$

Lastly, the cost of hydrogen transport via trucks (C_{Trucks}^{VOM}) was calculated using Equation 3.36 and was obtained in €/MWh [40]. Here, the driving distance from Port of Gothenburg and Göteborg Landvetter Airport was estimated to be 29 km one way trip while the driving and loading/unloading cost for year 2050 were taken from [45] as 0.048 $€_{2020}$/MWh and 1.85 $€_{2020}$€/MWh respectively. These costs include both operational and investment costs.

$$C_{Trucks}^{VOM} = Distance \cdot Driving\ Cost + Loading/Unloading\ Cost \tag{3.36}$$

3.3.2 Technical Parameters

Table 3.5 shows the selected parameter data for technologies and units for local generation of electricity. The electric consumption for the liquefaction plant (ε_{Liq}) was calculated by using Equation 2.1 presented in Section 2.1.2 where an average

electric consumption was estimated for capacities between 20 and 200 tpd. The electric consumption of the compressors (ε_{comp}) was calculated using Equation 2.2 presented in Section 2.1.4.

Table 3.5: Parameter data for technologies and local generation of electricity.

Technologies	$\varepsilon \left[\frac{MWh_{el}}{MWh_{H_2}}\right]$	T [years]
Electrolyzer [57]	1.33	35
Liquefaction [27]	0.26	40
Pipeline [45]	-	50
Trucks [45]	-	10
Compressor 1 [40] [63]	0.022	10
Compressor 2 [40] [63]	0.029	10
Cable	-	-
Generation	ε	T [years]
Wind power [62]	-	30
Solar PV [62]	-	40

Table 3.6 shows the selected parameter data for storage units of hydrogen and electricity. All technical data for the pressurized H_2 tank of type IV was based on data for type I, except for the discharge rate ($\gamma^{disch}_{H_2Tank}$) that was assumed to not be a limiting parameter and was set to 1, given the lack of available data. The charge efficiency of the cryogenic tank ($\eta^{ch}_{LH_2Tank}$) was also assumed to be equal to the discharge efficiency ($\eta^{disch}_{LH_2Tank}$) due to the last mentioned reason. On the other hand, hydrogen storage in LRC is not available in industrial scale so several assumptions were made for the selection of the parameter data. Charge/discharge rates were based on data from Skallen [36] where natural gas is stored. Charge and discharge efficiencies were based on data for hydrogen storage in salt caverns. Moreover, hydrogen losses during storage were neglected.

Table 3.6: Parameter data from the literature for storage of hydrogen and electricity.

Storage	Unit	H_2 Tank [61]	LH_2 Tank	Battery [61]	LRC
η^{ch}_S		0.9	0.9 [64]	0.985	0.99 [61]
η^{disch}_S		1.0	0.9 [64]	0.975	1.0 [61]
δ_S	[%/h]	0	$1.25{\cdot}10^{-3}$ [27]	0.041	-
T	[years]	20	30 [27]	30	30 [34]
γ^{ch}_S	$\left[\frac{\text{MWh}_{ch}}{\text{MWh}_{cap}}\right]$	0.0048	0.33 [30]	0.50	0.0020 [36]
γ^{disch}_S	$\left[\frac{\text{MWh}_{disch}}{\text{MWh}_{cap}}\right]$	1.0	2.0 [30]	3.0	0.0056 [36]

3.3.3 Space Requirements

The space requirement for the hydrogen storage alternatives is based on the volume of the maximum stored hydrogen, according to Equation 3.37, where e^{H_2} is the lower heating value of hydrogen expressed as energy per mass and ρ is the density of hydrogen at the required storage pressure and phase. The used values are presented in Table 3.7.

$$Volume_{\beta} = \frac{Cap_{\beta}}{e^{H_2} \cdot \rho} \tag{3.37}$$

Table 3.7: Densities for hydrogen for storage pressure and temperature [65].

	ρ [kg/m^3]
H_2 (@200 bar, 20 °C)	14.7
H_2 (@850 bar, 20 °C)	45.1
LH_2 (@1 atm, -252.8 °C)	70.9

The area needed for the liquefaction process ($Area_{Liq}$) was calculated from a correlation shown in Equation 3.38 which is taken from HDSAM [27]. Here, the capacity of the liquefaction process (Cap_{Liq}) should be expressed in tpd. For the local electricity production, the space requirements were calculated based on data from Danish Energy Agency. For wind power, the factor 417 m^2/MW was used which is based on a space requirement in form of a square with a 50 m length [62]. The area required for the utility scale solar PVs was calculated based on the factor 10840 m^2/MW [62].

$$Area_{Liq} = 25000 \cdot \left(\frac{Cap_{Liq}}{30}\right)^{0.6} \tag{3.38}$$

3.3.4 Cost of Aviation Fuels

To compare the cost of electricity, compressed hydrogen and liquid hydrogen the marginal cost is taken out from the model runs. However, to be able to get a marginal cost for all the hours of the year, the demand must be greater than zero for hydrogen in gaseous and liquid phase. Otherwise, the constraint is not active and no marginal cost will be calculated for those timesteps in GAMS. Therefore, a small demand of 0.1 kWh was added to the hydrogen demands, to ensure activation of constraints for every timestep. By adding a small demand, the Right Hand Side (RHS) marginal cost is obtained.

Another way of representing the cost is to weigh the marginal cost relative to the consumption since the average marginal cost is not necessarily representative of the marginal cost during hours with demand. The consumption based cost was calculated according to Equation 3.39, where MC_t^{fuel} is the marginal cost for the different aviation fuels, electricity, compressed hydrogen and liquid hydrogen. D_t^{fuel} is the consumption of the fuel and C_{fuel} is the average cost of the fuel.

$$C_{fuel}\left[\frac{€}{\text{MWh}}\right] = \frac{\sum_t MC_t^{fuel} \cdot D_t^{fuel}}{\sum_t D_t^{fuel}} \tag{3.39}$$

3.4 Sensitivity Analysis

The effect of several technology limitations on the total system cost was investigated. Firstly, only separate limitations were performed, including a cable limited to a capacity of 12 MW and 0 MW respectively, the removal of flexible charging and two scenarios where local electricity generation was limited to only wind power or solar PVs. Göteborg Landvetter Airport has currently a contract on a maximum power supply to cover their own operation. If the maximum power supply is not allowed to be increased from today's level, the airport needs to supply the new load without relying on the grid which is represented by a 0 MW cable. However, the airport has a redundant cable with a capacity of 12-14 MW that could be used, which laid the foundation for the second limitation that was used in the sensitivity analysis. Similarly, wind power and solar PVs are two technologies that are uncertain if they can be implemented due to safety concerns. The removal of the flexible charging of airplanes during night was investigated since it can be impractical for implementation due to lack of labour or fire hazard. The influence on installed capacities of the electrolyzer, compressors, wind turbines, solar PVs and the cable connection to the grid was also analyzed. Similarly, the effect of double limitations was also investigated, including scenarios with no wind power and cable limitations, no solar PVs and cable limitations and a scenario with no local electricity generation. Lastly, each storage option was actively excluded separately from the energy system and their influence on the system cost was studied. The LRC storage was excluded due to uncertainties of the geological conditions close to the airport. The pressurized vessels and the cryogenic tank were excluded due to uncertainties in technology developments and implementation in large scale.

In this project, the hydrogen market price was taken as a constant value of 110 $€_{2020}$/MWh which is an uncertain parameter that plays a crucial role in determining the cost-effectiveness of the hydrogen import via pipeline and trucks. The hydrogen price was decreased successively until the breaking point occurred where hydrogen import was introduced in the cost optimal solution.

Other uncertain parameters that were varied are the specific investment of the liquefaction plant and the boil off losses from the cryogenic tank. Then, the effects on the total system cost and installed capacity of technologies were examined in order to analyze the robustness and behavior of the energy system. The investment costs were systemically varied between 50% and 250% of the initial investment cost. The daily boil off losses were varied between 0% and 5% in order to account for the uncertain interval given in the literature [25].

4

Results

The following sections will present the main results obtained from each study case including distance profiles (4.1), how the electricity and hydrogen demand is supplied (4.2) and the performed sensitivity analysis where the impact of different cost assumptions was assessed (4.3).

4.1 Electricity and Hydrogen Demand

From the mapping of the departing flights from Göteborg Landvetter Airport, the hydrogen and electricity demands were estimated for three different scenarios of direct and indirect electrification, based on the current amount of passenger flights. The annual quantity of electricity, compressed hydrogen and liquid hydrogen demand in terms of mass (kton) and energy (GWh) are presented in Table 4.1 and 4.2 for each case.

Table 4.1: Annual amount of hydrogen demand for each case.

	H_2 [kton]	LH_2 [kton]
Case 1	11	8.1
Case 2	5.0	16
Case 3	0	21

Table 4.2: Annual amount of electricity and hydrogen demand for each case.

	Electricity [GWh]	H_2 [GWh]	LH_2 [GWh]
Case 1	30	250	270
Case 2	0	170	520
Case 3	0	0	680

The distance profile for flight ranges up to 400 km is presented in Figure 4.1. These distances were covered by the battery-electric aircraft in Case 1 and hydrogen powered aircraft in Case 2 and 3. The hourly demand is presented over a one year period. The demand varies over the quarters with the lowest demand during the

first quarter of the year (Q1) which corresponds to 24% and the highest demand during the second quarter (Q2) which makes up 27% of the yearly demand.

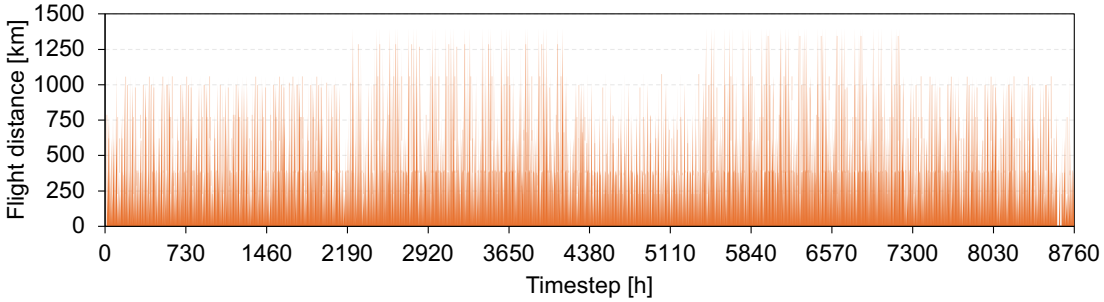

Figure 4.1: The hourly distance profile for flight range 0-400 km.

The distance profile for flight ranges above 400 km and below 800 km can be seen in Figure 4.2. This range is covered by hydrogen powered aircraft in all cases, more specifically gaseous hydrogen in Case 1 and 2 and liquid hydrogen in Case 3. The lowest hydrogen demand can be found in Q1 which corresponds to 22% of the yearly demand and the highest in Q2 and Q3 (third quarter) with 27% for each period.

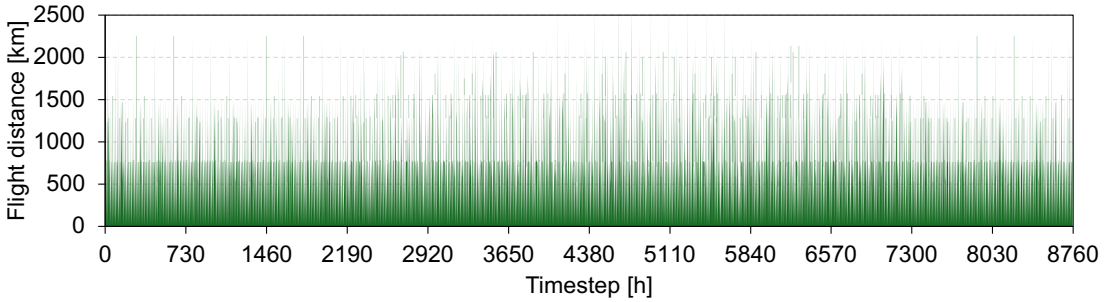

Figure 4.2: The hourly distance profile for flight range 400-800 km.

The hourly distance profile for flight ranges above 800 km and below 1500 km is shown in Figure 4.3. This range is covered by gaseous hydrogen in Case 1 and liquid hydrogen in Case 2 and 3. The lowest demand occurs in Q1 which stood for 23% of the demand. The highest hydrogen demand occurs during Q2 and Q3 where 26% of the yearly demand is found in each period.

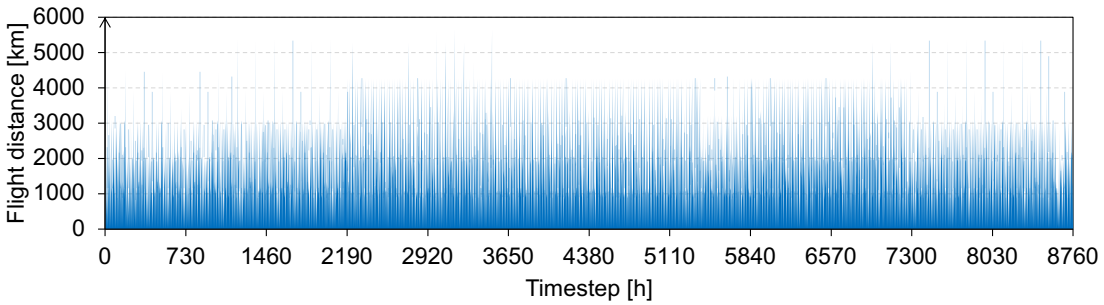

Figure 4.3: The hourly distance profile for flight range 800-1500 km.

For flight ranges above 1500 km and below 3100 km, the hourly distance profile is shown in Figure 4.4 which is covered by liquid hydrogen for all cases. This distance profile is the most season-dependent where the highest liquid hydrogen demand can be found in Q2 and Q3 which corresponds to 29% and 37% of the yearly demand respectively. The lowest demand occurs during the first quarter corresponding to 14% of the yearly demand.

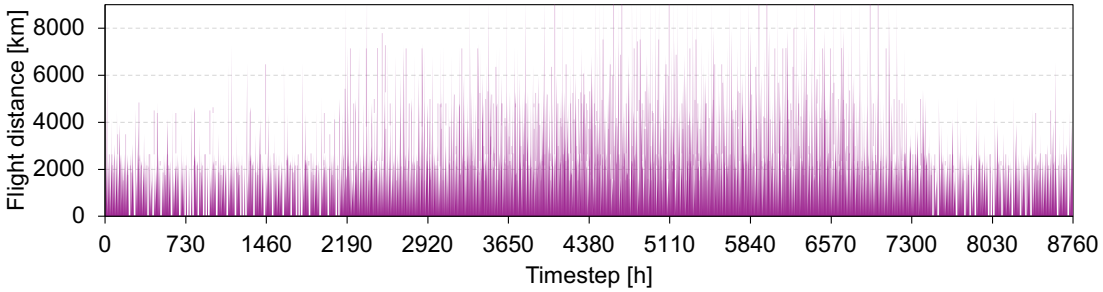

Figure 4.4: The hourly distance profile for flight range 1500-3100 km.

Figure 4.5 shows an example how the distance profile can look for distances up to 3100 km, based on flight data taken for 8 days in January. From the figure it can be seen that the travel distance during weekdays is similar due to regular commuter flights.There is also a reoccurring zero demand during night when the electricity prices are generally lower. Thus, flexible charging of airplanes was implemented.

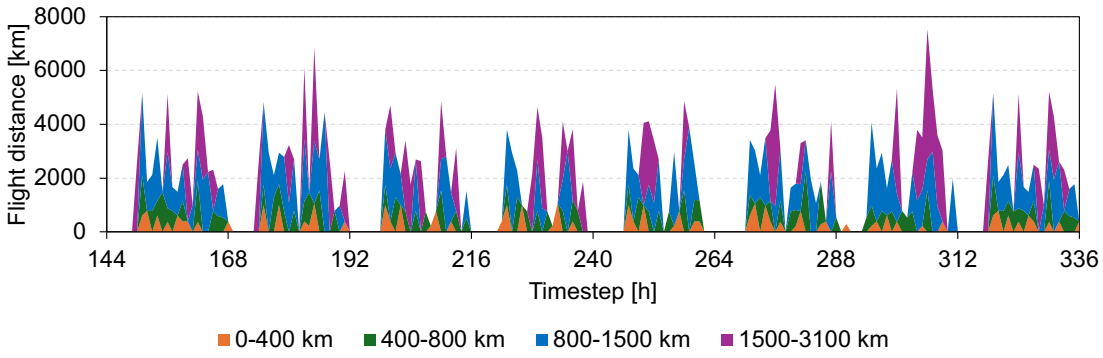

Figure 4.5: The hourly distance profile for flight ranges up to 3100 km for 8 days.

4.2 Electricity and Hydrogen Supply

The following sections will present the installed capacities of all technologies (4.2.1), load duration curves (4.2.2), running patterns (4.2.3), state of charge graphs (4.2.4), space requirements (4.2.5) and marginal prices (4.2.6) of electricity, compressed hydrogen and liquid hydrogen.

4.2.1 Installed Capacity

From the energy system model, the following installed capacities for the electrolyzer, liquefaction plant and compressors were found in the cost optimal solution as shown

in Figure 4.6. In all cases, the electrolyzer has a capacity between 120-131 MW, the liquefaction process between 50-102 MW, compressor 1 between 30-74 MW and compressor 2 between 0-157 MW hydrogen output. In Case 1, trucks appear with a maximum used capacity of 29 MW, however with low utilization where only 0.08% of the hydrogen demand is supplied with trucks during the modeled year. The highest increase occurs in the liquefaction process between Case 1 and Case 3. Moreover, it can be seen that compressor 1, still appears in Case 3, even if the energy penalty of compression before the liquefaction process is unnecessary from a process perspective, however needed for utilizing the LRC before liquefaction.

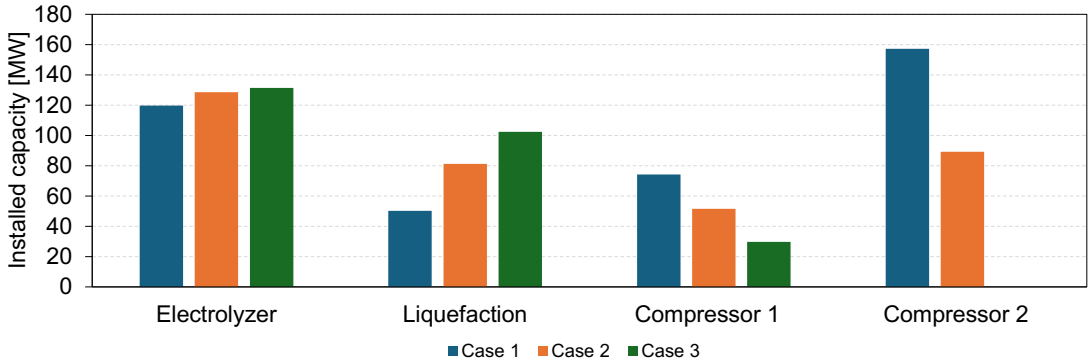

Figure 4.6: The installed capacities in the cost optimal solution for electrolyzer, liquefaction and compressors expressed in hydrogen output for Case 1, 2 and 3.

The cost optimal investment in electricity supply is presented in Figure 4.7. The highest rated power can be found in solar PVs for all three cases and the lowest for the cable connection to the grid.

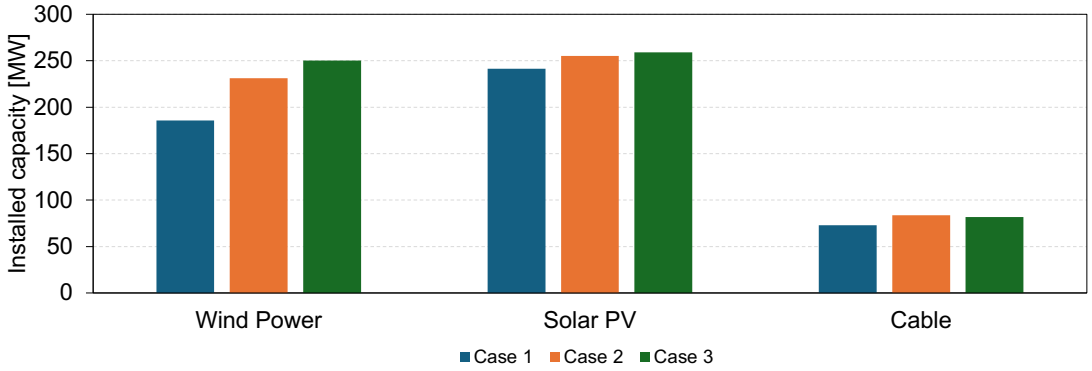

Figure 4.7: The installed capacities in the cost optimal solution for wind power, solar PVs and cable for Case 1, 2 and 3.

The electricity production as well as the electricity import and export can be seen in Figure 4.8. It can be seen that most of the electricity comes from onsite wind generation, ranging between 500 and 675 GWh during the year. Wind turbines can generate more electricity on a yearly basis with a lower installed capacity than solar PVs due to the higher average capacity factor of 0.31. The second largest electricity supply comes from the electricity grid, between 318-330 GWh. The lowest

contribution to electricity supply corresponds to solar PVs as shown in Figure 4.8, ranging between 260-279 GWh, which is due to the low average capacity factor of 0.12. Moreover, the exported electricity during the year is between 93-120 GWh.

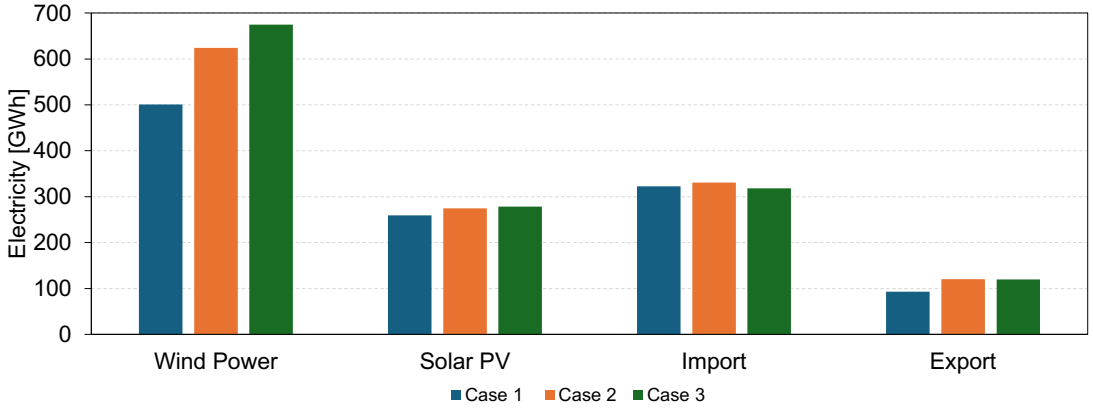

Figure 4.8: The produced and exported electricity in the cost optimal solution for Case 1, 2 and 3.

Finally, the cost optimal investment storage can be found in Figure 4.9. Note that the cost optimal solution does not result in battery investment for storage of electricity in any case. The liquid tank capacity increases by 40% between Case 1 and 3. Moreover, the LRC storage is still present in Case 3 although there is no gaseous hydrogen demand. This is due to the cost competitiveness of the LRC and the constant hydrogen flow that it can provide, making it possible for the liquefaction plant to operate at higher load for a higher amount of hours. Thus, the liquefaction plant can provide the same liquid hydrogen flow at a lower installed capacity. The other alternative would be import of hydrogen from external sites via trucks. However, at the assumed hydrogen market price in combination with the operational cost of trucks, the cost of importing hydrogen via trucks is very seldom cost competitive against onsite hydrogen production with storage. This resulted in trucks only being utilized in Case 1 and only supplying a small share of the yearly hydrogen demand (0.08%) and none in Case 2 and 3.

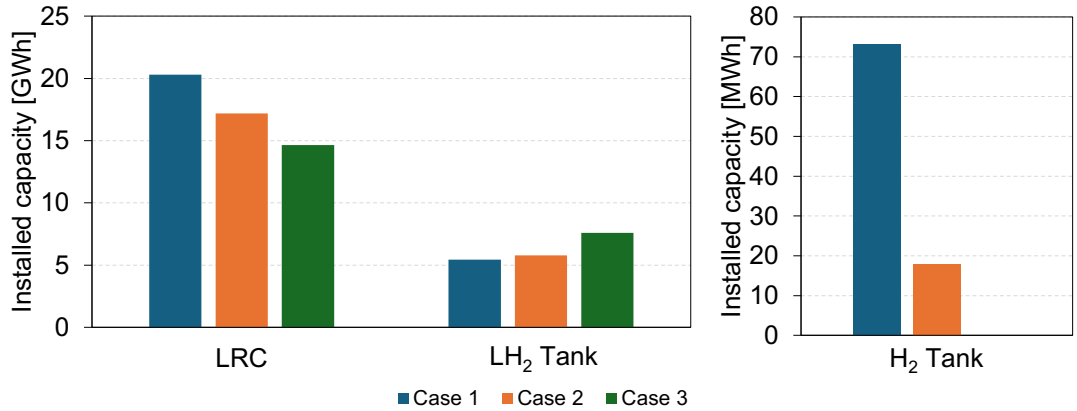

Figure 4.9: The installed capacities in the cost optimal solution for LRC, cryogenic tank and the pressurized vessel for Case 1, Case 2 and Case 3.

4.2.2 Load Duration Curves

The following section will present the load duration curves for the liquefaction process and electrolyzer in order to compare the operating load for gaseous hydrogen and liquid hydrogen in the modeled energy system. Similar graphs for compressor 1 and 2 and import/export of electricity can be found in Appendix C.

The load duration for the liquefaction process for the three different cases can be seen in Figure 4.10. In Case 1, the liquefaction processes runs at an average load of 69% of its maximum capacity and at maximum load for 5500 hours. The hours the liquefaction process runs at zero load correspond to high electricity prices in combination with low local electricity production. For Case 2 and Case 3, the average operating loads are 79% and 82% of its maximum capacity. In Case 3, a plateau can be seen around timestep 6570 with an operating load of 82 MWh/h, which corresponds to the maximum discharge rate of LRC with the capacity installed in this case and the recirculated boil-off losses.

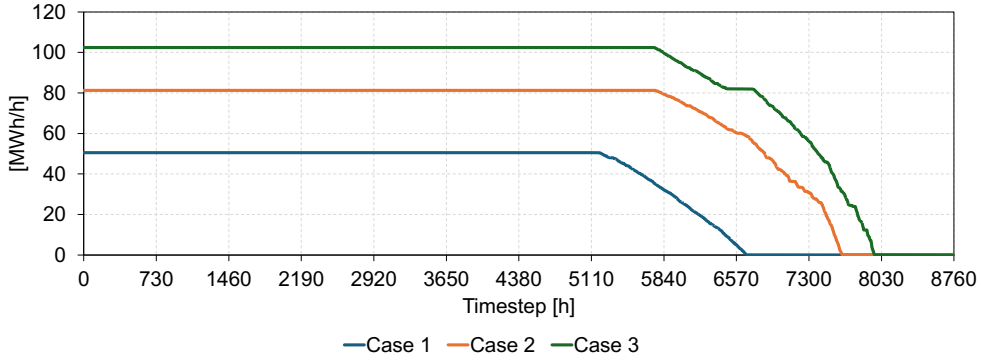

Figure 4.10: The load duration for the produced LH_2 from the liquefaction plant.

In the load duration graph for the electrolyzer in Figure 4.11, it can be seen that for all three cases, there are approximately the same amount of hours the electrolyzer runs at its installed capacity, which corresponds to the hours with high local electricity production. Similarly, the amount of hours without hydrogen production is almost the same for all cases, which corresponds to hours of low local electricity production in combination with high electricity prices. In Case 1, 2 & 3, the average operating load over the year is 62%, 63% and 62% of the maximum capacity.

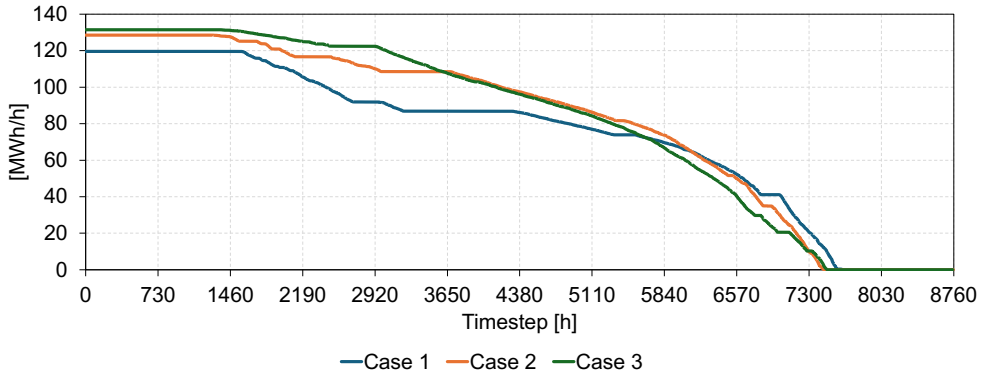

Figure 4.11: The load duration for the produced H_2 from the electrolyzer.

In the load duration curves for the electrolyzer and liquefaction, it can be seen that for all cases the liquefaction process operates at its maximum load for more hours in comparison to the electrolyzer. This is due to the higher investment cost as well as the lower electricity consumption of liquefaction in comparison to the electrolyzer. Thereby the liquefaction process is less sensitive to variation in electricity supply and produces at its maximum capacity for more hours.

4.2.3 Demand and Supply of Electricity

The electricity consumption of the electrolyzer, liquefaction plant, compressors, electric aircraft and the sold electricity are presented Figure 4.12 for an example time period of 8 days in January. Here BEA stands for the electricity required for charging of battery-electric airplanes. The electricity demand is supplied by wind power, solar PVs and the electricity import from the grid, which is presented in Figure 4.13. The electrolyzer consumes the largest amount of electricity and produces at generally high load, except for hours when there are high electricity prices and/or low electricity generation of electricity onsite. On the other hand, the liquefaction plant produces at a generally more constant load in comparison to the electrolyzer. In other words, the electrolyzer responds earlier to variations in electricity prices and supply. Moreover, during hours of high electricity production from wind power and solar PVs, the liquefaction plant operates generally at full load. However, a combination of high electricity prices and low electricity production results in no operating load in the liquefaction plant.

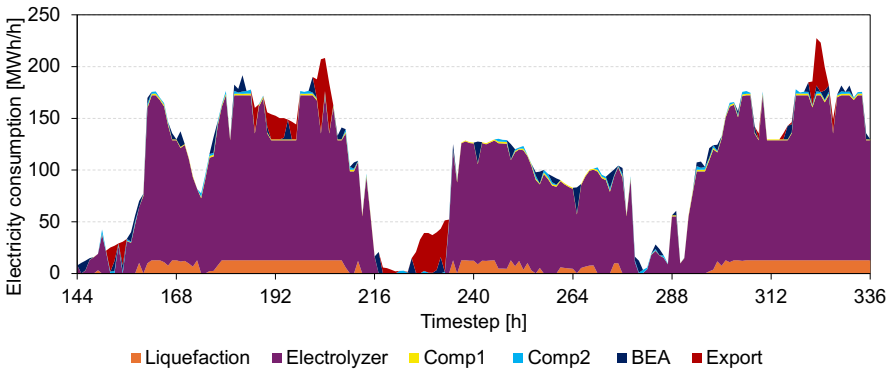

Figure 4.12: Electricity consumption of different units during 8 days.

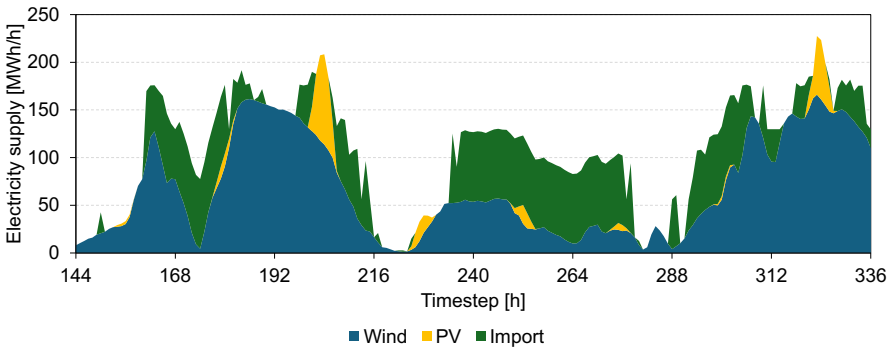

Figure 4.13: Electricity supply of different units during 8 days.

There is no curtailment of electricity during the period presented in Figure 4.12 and 4.13, but it occurs during summer when there is overproduction of electricity from the solar PVs. Individual profiles for these 8 days can be found in Appendix E.

4.2.4 State of Charge

The time that every storage can supply the system with hydrogen or electricity is presented in Table 4.3. For Case 1, the LRC storage can supply the system with hydrogen for approximately 10 days, while the pressurized vessels only last for a couple of hours. This behavior is due to several factors. The LRC storage has a lower investment cost per energy which makes it profitable to invest in large storage volumes, despite low discharge and charge rates. On the other hand, the pressurized vessels store hydrogen at a higher pressure and can be discharged faster than the LRC. However, the cost optimal solution includes a low installed capacity due to high investment cost. As for the cryogenic tank, it has also a fast charge and discharge rate, but the investment cost per energy is also much lower in combination with a high investment cost for the liquefaction plant. Thus, it is cost optimal to invest in larger volumes that can supply the system with liquid hydrogen for several days. The model does not invest in batteries for Case 1, 2 and 3.

Table 4.3: The time that the storage can supply the average hydrogen demand.

	LRC [days]	H_2 tank [h]	LH_2 tank [days]
Case 1	10.3	1.8	5.5
Case 2	9.2	1.0	4.1
Case 3	7.8	0	4.1

From the state of charge for the LRC shown in Figure 4.14, it can be seen that around timestep 750, the storage is completely empty. This corresponds to a long period of high electricity price (see Figure 3.2) in combination with a relatively low local electricity production. The second time of the year the LRC is completely emptied in all of the cases is during Q4 (fourth quarter) when the electricity prices are relatively high and the local production from solar PVs and wind power is low. In Case 3, the storage is completely emptied around hour 5300, which corresponds to period Q3 with a high LH_2 demand.

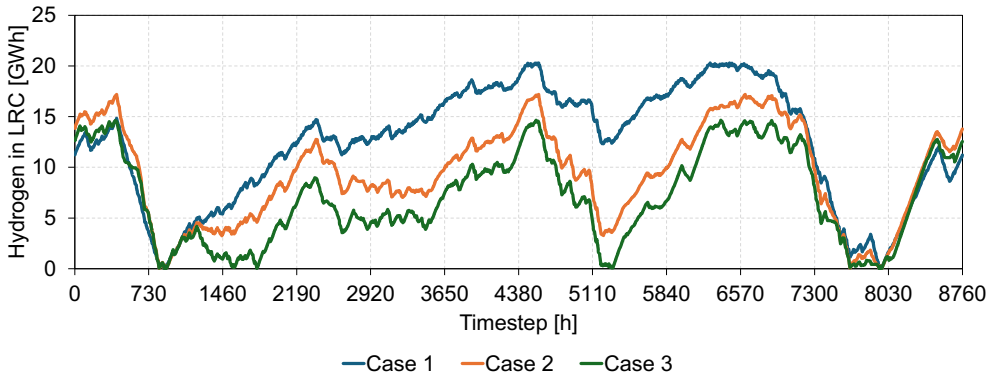

Figure 4.14: State of charge for LRC storage.

The state of charge for the compressed hydrogen tank is shown in Figure 4.15, where it can be seen that the tank is emptied during the same periods as the LRC, which can again be explained by the high electricity prices and low onsite electricity generation during those hours. The compressed hydrogen tank has a low installed capacity and can only cover around 1 hour of the average hydrogen demand, but at the same time it has a fast charge and discharge rate. This results in 30 cycles for Case 1 and 22 cycles for Case 2 over the entire year for the pressurized tank storage.

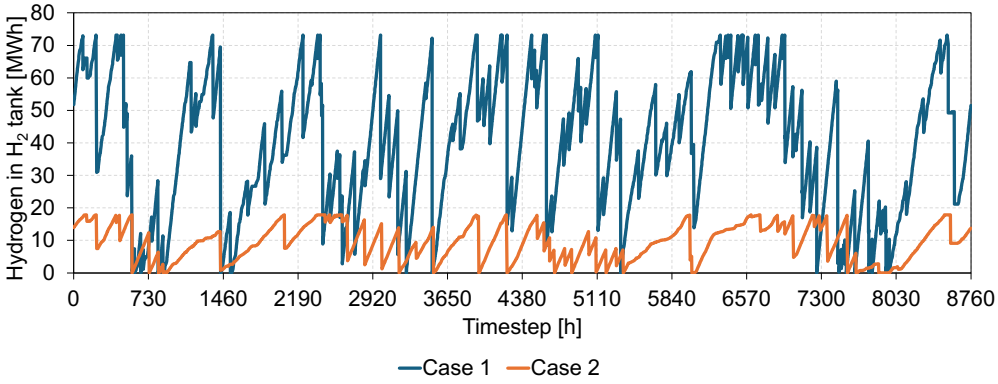

Figure 4.15: State of charge for pressurized vessel storage.

Figure 4.16 shows the state of charge for the cryogenic tank which has a larger installed capacity than the compressed hydrogen tank, thus resulting in fewer cycles. The highest peaks occur during Q2 in order to be able to supply hydrogen during the high demand peaks in Q3. The level proceeds to 0 around timestep 5490 which corresponds to the start of Q3. The storage is then charged to higher levels during Q4 and then completely emptied during Q1 at timestep 835 due to a period of high electricity prices and low electricity production.

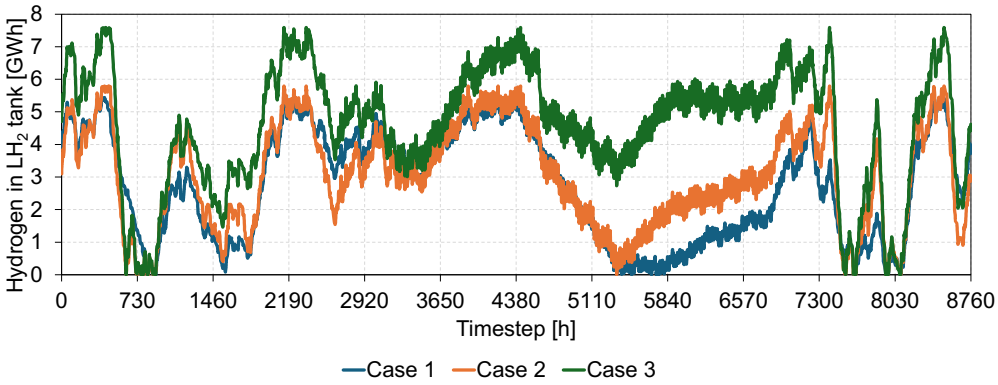

Figure 4.16: State of charge for the cryogenic tanks storage.

4.2.5 Space Requirement

The space requirements for the electrolyzer, liquefaction plant, wind farm, solar PVs, LRC, H_2 tanks and LH_2 tank were calculated and are presented in Table 4.4 and 4.5. The largest area is required by the solar PVs due to their low power output per area,

thus requiring a large number of cells. It can also be observed that the liquefaction plant takes up a 23 times larger area than the electrolyzer in Case 1. The space required by the storage units is based on the volume taken up by hydrogen which in practice means that the space requirement is larger.

Table 4.4: Required area for the hydrogen and electricity units.

	Case 1 [m^2]	Case 2 [m^2]	Case 3 [m^2]
Electrolyzer	1 200	1 300	1 300
Liquefaction	28 000	37 000	43 000
Wind farm	77 000	96 000	100 000
Solar PV	2 600 000	2 800 000	2 800 000

Table 4.5: Required volume for the storage units.

	Case 1 [m^3]	Case 2 [m^3]	Case 3 [m^3]
LRC	43 000	36 000	31 000
H_2 Tank	49	12	0
LH_2 Tank	2 300	2 500	3 200

4.2.6 Cost of Aviation Fuels

The marginal cost for the investiagted aviation fuels is presented in Table 4.6. It can be seen that the average marginal cost is 49 €/MWh for electricity, 52-54 €/MWh for compressed hydrogen and 74-78 €/MWh for liquid hydrogen.

Table 4.6: Average marginal cost of electricity for aviation fuels.

	Case 1	Case 2	Case 3
Electricity [€/MWh]	49	49	49
H_2 [€/MWh]	53	53	54
LH_2 [€/MWh]	74	78	78

The average consumption based cost for the investigated aviation fuels is presented in Table 4.7. The electricity consumed by the battery-electric aircraft has an average cost of 49 €/MWh. Compressed hydrogen has an average consumption weighted cost of 64-65 €/MWh and liquid hydrogen between 85-90 €/MWh.

Table 4.7: Consumption based cost for aviation fuels.

	Case 1	Case 2	Case 3
Electricity [€/MWh]	49	-	-
H_2 [€/MWh]	64	65	-
LH_2 [€/MWh]	90	86	85

4.3 Sensitivity Analysis

The following sections will present the results from the performed sensitivity analysis regarding technology limitations (4.3.1) and parameter variations (4.3.2).

4.3.1 Technology Limitations

The energy system was investigated by adding constraints regarding allowed installed capacity of technologies and storage for all cases. Figure 4.17 shows how the system cost is affected by the implementation of single limitations such as limiting the capacity of the electrolyzer, wind power, solar PVs and the cable. Figure 4.18 shows the distribution of installed capacities between the different technologies and storage units for each of the single limitations in Case 1. If the model is not allowed to invest in the electrolyzer unit, the demand will be met by importing hydrogen via pipeline and trucks which results in a 99% increase of the system cost in Case 1, 98% in Case 2 and 94% in Case 3. This is however highly dependent on the set hydrogen market price of 110 $€_{2020}$/MWh. Since the biggest electricity consumer is the electrolyzer which is not present in this scenario, the installed wind power, solar PVs and cable decreased by at least 80%.

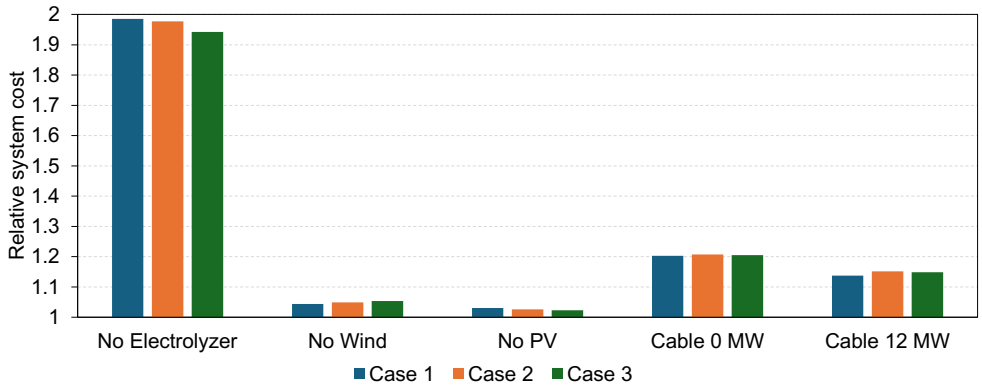

Figure 4.17: The effect of separate limitations on the system cost.

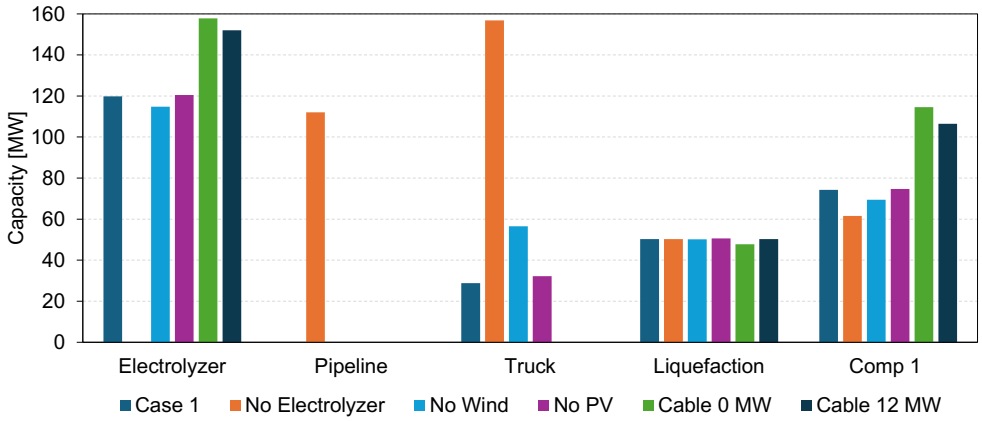

Figure 4.18: The effect of separate limitations on the installed capacity of technology units in Case 1.

In a case where electricity production through local wind power or solar PVs is not allowed, the system cost increased by 4% and 3% respectively for Case 1. The biggest difference between these two scenarios is that the maximum used capacity of trucks is higher if wind power is not allowed as shown in Figure 4.18. When no wind turbines are allowed onsite, the installed capacity of solar PVs increased by 65% and the cable by 69%. However, when a case with no solar PVs is investigated, the cable increased by 8% and the installed wind turbines capacity increased by 40%.

If the airport is not allowed to increase the cable capacity from today's level, the new load should be supplied without relying on the grid. This is represented as a case where the cable is set to zero, which resulted in an increased system cost by 20% for all cases, as shown in Figure 4.17. In order to compensate for the cable, the local electricity production increased by 30% for solar PVs and 90% for wind power. When the cable capacity was limited to 12 MW, and thereby limiting the electricity import and export to 12 MWh/h, the system cost increased by 13% in Case 1 and 15% in Case 2 and 3. The limitation resulted also in an increase of 18% in solar PV capacity and 66% in wind power capacity. Moreover, the electrolyzer capacity increased by 23% as shown in Figure 4.18.

The percentage change in installed capacity for the different technologies for Case 2 and 3 are presented in Appendix D.1 and follow a similar trend as for Case 1 in Figure 4.18. The biggest difference is the maximum utilized capacity of trucks which decreases from 157 MW in Case 1 to 0 MW in Case 3 for a case without onsite production of hydrogen. Trucks mainly appear when compressor 1 is running at maximum capacity as it is more cost effective to import hydrogen via trucks than to increase the compressor size. Trucks also appear during hours with high electricity prices and low onsite electricity production, thus avoiding electricity consumption in compressor 1. However, Case 3 has a demand of only liquid hydrogen meaning that for a scenario without onsite production of hydrogen, it is not profitable to invest in LRC. Hence, trucks disappear due to the absence of LRC storage in combination with the higher variable operating cost in comparison to pipeline.

Figure 4.19 shows how the system cost is affected by implementing limitations such as no wind power and/or solar PVs in combination with a cable limitation. The y-axis shows the total system cost relative to the initial system cost. The x-axis shows the limitation for each case. Figure 4.20 shows the distribution of the installed capacities between the different technologies and storage units for the combined limitations in Case 1. By investigating a case with no electricity import/export in combination with no local wind, the system cost increased by 67% in Case 1. This increase could be explained by the fact that the imported electricity from the grid has a high share of wind and therefore the low electricity prices often correspond to high local wind production. The investment in PVs corresponds to a 349% increase in capacity, which in this scenario is the only option for electricity supply. The electrolyzer capacity increased by 105% and compressor 1 by 161% as shown in Figure 4.20. These capacity increases are due to the lower average capacity factor of solar PVs, the generation of electricity being concentrated during some hours of the day and the uneven distribution of solar power over the year. Moreover, The LRC storage capacity increased by 209% and the LH_2 tank decreases by 16%. In a similar

scenario where wind power is not allowed close to the airport in combination with a cable connection limited to 12 MW, the system cost increased between 48-54%.

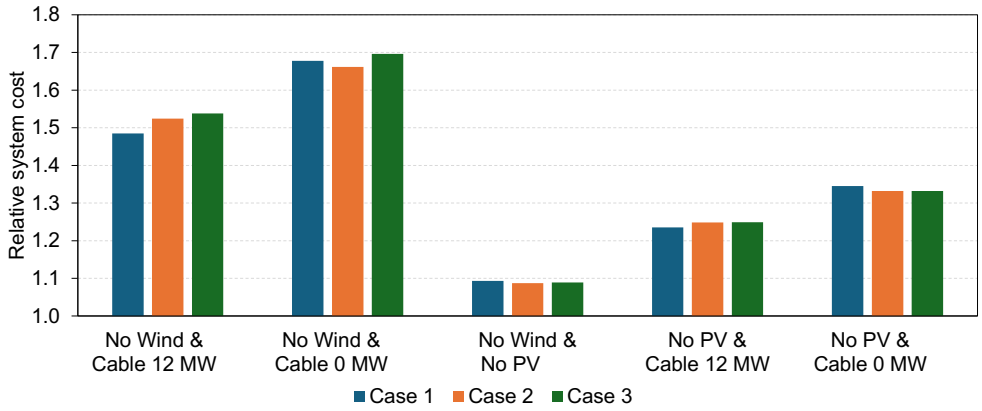

Figure 4.19: The effect of double limitations on the system cost.

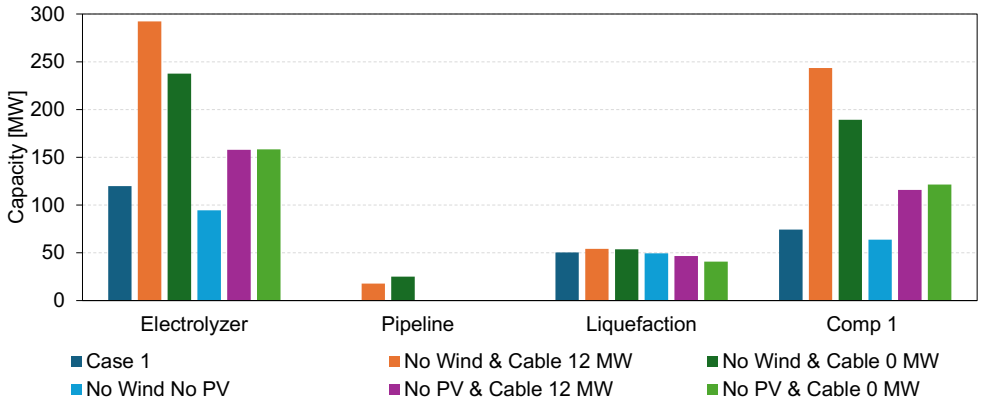

Figure 4.20: The effect of double limitations on the installed capacity of technology units in Case 1.

In a scenario with no solar PVs and 0 MW cable, meaning that the entire electricity demand is supplied by wind power, the system cost increased by 34% in Case 1 which is a smaller increase than a case where the entire electricity demand is supplied by solar PVs. This could be explained by the higher average capacity factor of wind turbines and the more even distribution of electricity over the year, when compared to solar PVs. In a similar scenario where solar PVs are not allowed close to the airport in combination with a cable connection limited to 12 MW, the system cost increased by 24% in Case 1, as shown in Figure 4.19.

If both wind power and solar PVs are not allowed, the system cost increases by approximately 9% for all cases. The entire electricity demand in this scenario is provided by the cable connection to the grid, thus the capacity of the cable is doubled as can be seen in Figure 4.20. The majority of hydrogen is supplied by the electrolyzer while the rest is imported via trucks.

In Case 1, it is assumed that the airplanes standing over night can be charged during the night as long as the load is fulfilled before the airplanes leave in the morning. A

case where this flexibility is not an option, the system cost increases by 0.2% which is minimal and it is therefore not shown in the graphs. The installed capacities were very similar to Case 1 with flexible charging, however, with the exception of the maximum used trucks during the year that increased by 27%.

The percentage change in installed capacity for the different technologies for Case 2 and 3 are presented in Appendix D.2 and follow a similar trend as for Case 1 in Figure 4.20. The biggest difference occurs for the scenarios with no wind power and a cable limitation. In Case 1, it can be seen that the installed capacity of the electrolyzer and compressor 1 is bigger in a scenario with no wind and a cable limited to 12 MW than a scenario with no wind and a cable limited to 0 MW. However, the opposite occurs in Case 2 and 3, meaning that the installed capacity of the electrolyzer and compressor 1 is higher in the scenario with no local wind power and cable connection to the grid.

From the model runs, it can be seen that compressor 1 has the same capacity as the maximum charging capacity of the LRC for Case 3 independently of single and double limitations. This could be explained by the sole purpose of compressor 1 in Case 3 which is to increase the pressure of hydrogen in order to store it in the LRC before the liquefaction plant. Hence, there is no advantage in having a higher capacity for compressor 1. However, in Case 1 and 2, compressor 1 always has an installed capacity higher than the maximum charge rate of the LRC. These cases have a demand of compressed hydrogen meaning that the compressor here also provides another purpose, resulting in a higher installed capacity of compressor 1.

Figure 4.21 shows how the system cost is affected by excluding one storage option. The liquefaction process can operate flexible due to the cryogenic tank. If the tank is removed, the liquefaction plant must operate after the liquid hydrogen demand. By doing so, the system cost increases by 80% for Case 1. This investment increase originates from the increased capacity of the liquefaction process which increased by 500%, since the capacity of the liquefaction process must be able to produce the highest hourly liquid hydrogen demand occurring during the year. The cost optimal solution also has an increased capacity of compressor 1 with 64%. The most affected case from removing the cryogenic tank was Case 2, where the system cost increased by 98%. This could be explained by the increased capacity of the liquefaction process which increased by 418% and the LRC which increased by 124%.

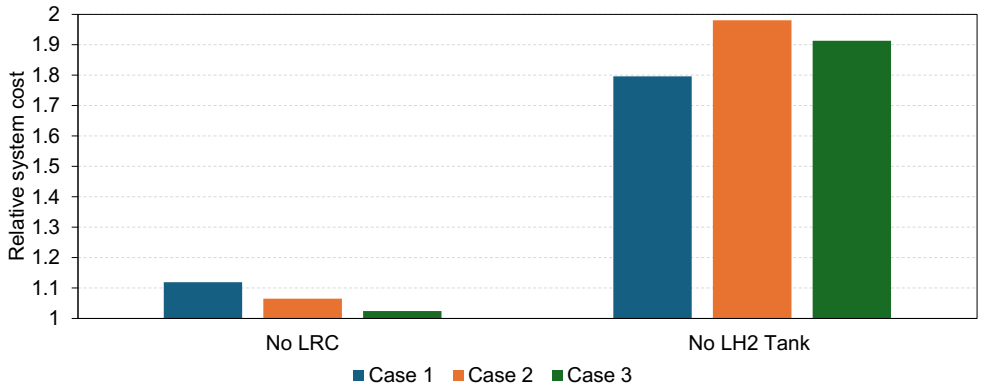

Figure 4.21: The effect of excluding one storage option on the system cost.

Another storage option which offers flexibility for the liquefaction process is the LRC. By considering an option where LRC is not a storage alternative, the system cost increased by 12% in Case 1, 7% in Case 2 and 2% in Case 3. In Case 1, the cost optimal solution included an increase of maximum utilized capacity of trucks by 410%. On the other hand in Case 3, the absence of the LRC is compensated by a 200% larger cryogenic tank, 22% larger cable and a 17% smaller electrolyzer.

In a scenario where the compressed hydrogen storage is excluded, the system cost increased by 1%, where the increase in cost comes mainly from a 30% larger compressor 2 and 130% increase in maximum utilized truck capacity.

4.3.2 Varying Key Parameters

A sensitivity analysis was performed for the hydrogen market price, by varying the price in order to find the breaking point where hydrogen begins to be imported. The cost optimal solution in Case 1 already includes import of hydrogen via trucks. The breaking point occurs at a hydrogen price of 279 €/MWh. However at the assumed market price, only 0.08% of the hydrogen was imported with trucks. In the modeled energy system, import of hydrogen via trucks is used as a peak technology with the characteristic of a high operating cost and a low investment cost. This can be explained by the trucks investment being included in the variable operating cost. In Case 2 and 3, the breaking point for import of hydrogen via trucks occurs at 103 €/MWh and 107 €/MWh respectively. However, import of hydrogen via pipeline occurs at lower hydrogen prices. In Case 1 it occurs at prices lower than 64 €/MWh, in Case 2 lower than 71 €/MWh and in Case 3 lower than 74 €/MWh.

Figure 4.22 shows how the total system cost and installed capacity of the liquefaction plant vary when the investment cost of the liquefaction plant is increased up to 300% as well as decreased down to 30% of the initial cost in Case 3. The graph shows that the system cost is linearly dependent on the change in the liquefaction investment cost. Additionally, the capacity of the liquefaction plant decreased as the investment cost increased.

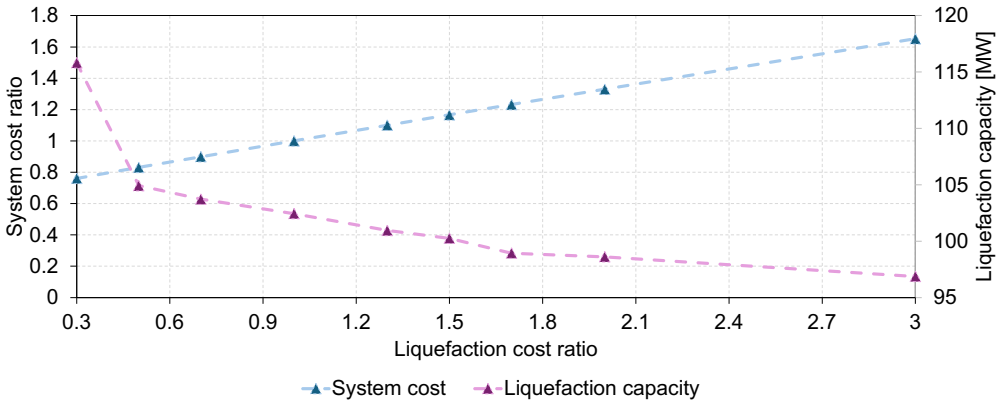

Figure 4.22: The effect of the investment cost of the liquefaction plant on the system cost and liquefaction plant capacity.

Figure 4.23 shows that a more expensive liquefaction plant leads to a larger installed

LRC and cryogenic storage in order to limit investment in the liquefaction plant, which in turn leads to a decreased electrolyzer capacity. However, as the cost of the liquefaction plants decreases below 100% of the initial cost, the capacity of the cryogenic tank starts increasing again. This could be explained by the fact that the liquefaction plant is sufficiently cheap in order to increase its capacity and consecutively produce large amounts of liquid hydrogen when the electricity prices are low. Therefore, the capacity of the cryogenic tank starts increasing again in order to store the produced liquid hydrogen. In other words, the cryogenic tank is not there in order to limit the installed capacity of the liquefaction plant, but rather in order to store the amount of the liquid hydrogen produced during times of low electricity prices.

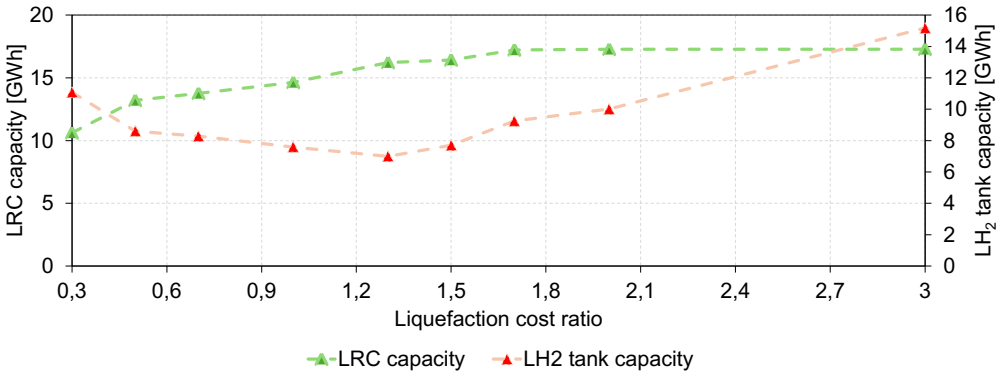

Figure 4.23: The effect of the investment cost of the liquefaction plant on the capacity of LRC and cryogenic tank.

According to the literature, boil-off losses from storage of liquid hydrogen in cryogenic tanks can reach up to 5% per day [25]. This parameter was therefore varied and the system cost ratio was plotted for each point as shown in Figure 4.24. This project uses a value of 0.03% per day, but if the boil off losses would increase to 5%, the system cost would be 1.5% higher. To compensate for the hydrogen losses, both the electrolyzer and liquefaction capacity increase which in turn leads to a lower storage capacity of the cryogenic tank.

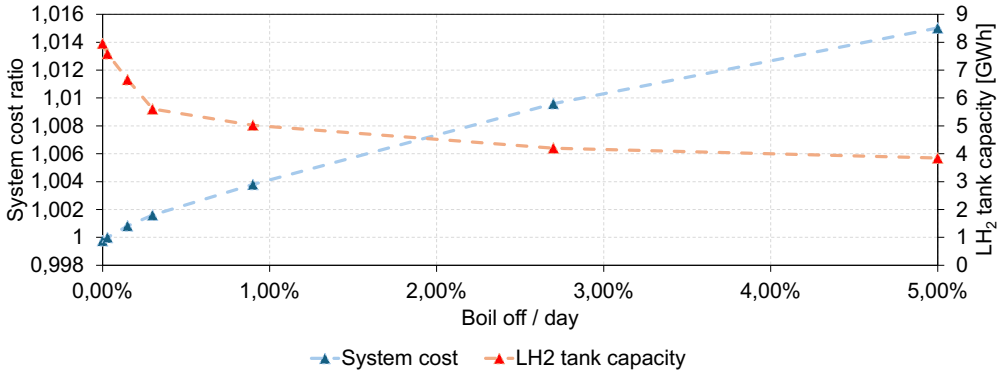

Figure 4.24: The effect of the daily boil off losses on the system cost and cryogenic tank capacity.

5

Discussion

From the mapping of the departures from Göteborg Landvetter Airport, it was found that the airplanes travel distance in the investigated flight ranges had a seasonal as well as a daily dependency. The chosen flight ranges for the aviation fuels will therefore affect the seasonal variation in the different fuel demands. The daily dependency will also be evident as almost no flights departure during nighttime. This implies that either the production needs to be flexible or that storage options need to be in place in order to manage the variation. Since it was found that several airplanes stand over night, it opens up the possibility for flexible charging of battery-electric airplanes during night and thereby increases the charging window in order to provide flexibility for the modeled energy system. Moreover, the electricity and hydrogen demand were estimated on the basis of the current aviation traffic departing from Göteborg Landvetter Airport. However, the aviation traffic is predicted to increase by 3-5% per year [2] which would affect the results.

The cost optimal solution of all three cases investigated in this project included supply of the direct and indirect electricity demand with a combination of wind power, solar PVs and import of electricity. It is economically beneficial to operate the electrolyzer when the electricity prices are low and local electricity production is high. Thus the model invests in different types of hydrogen storage which in turn increases the flexibility of the system and contributes to a lower system cost. Case 1 corresponds to the lowest energy demand since less liquid hydrogen is required while Case 3 has the highest.

From the model runs it was found that the increased electricity demand was fulfilled mostly by higher installed wind power capacity. Moreover, it was found that the system cost of the modeled energy system is highly dependent on allowing local wind power or increased connection to the electricity grid. If these two technologies were excluded from the system, the system cost increased by 66-69%. At the same time the solar radiation is highly concentrated during the middle of the day which results in a high electricity marginal cost for this system configuration. Therefore, in order to reduce the operational cost, the electrolyzer and compressor 1 are oversized. Even if this system resulted in a relatively high electricity cost, it was found to be cost optimal to produce the majority of hydrogen onsite while the rest was imported through pipeline at the assumed hydrogen cost of 110 $€_{2020}$/MWh. On the other hand, when the connection to the grid was limited simultaneously as the PVs, it resulted in an increased system cost by 33-34%. This means that all electricity production would come from onsite wind production, which has a higher

average capacity factor and therefore lower capacity is needed in order to supply the electricity demand. The installed wind power capacity could also provide electricity for more hours, which can be used to produce hydrogen via the electrolyzer. Thereby the electrolyzer is able to produce at a higher average operating load, resulting in a lower installed capacity.

The single technology limitations contributing the most to an increased cost is not allowing onsite hydrogen production which increased the system cost by 94-99%, followed by not allowing a cryogenic tank onsite which removes the flexibility of the liquefaction process and thus increased the system cost by 80-98%. However, the first result is highly dependent on the assumed hydrogen price which was set to 110 $€_{2020}$/MWh meaning that a lower market price would make hydrogen import a more viable option. These results also indicate that the storage options create a redundancy in the system which helps avoiding high electricity prices as well as allowing for a lower installed capacity to be able to provide the liquid hydrogen demand. Thus the implementation of storage, decreases the total system cost. Moreover, Figure 4.23 showed that a more expensive liquefaction process also leads to a larger cryogenic tank, validating its importance.

The liquefaction plant does in general avoid operation during low electricity supply and high electricity prices. However, the liquefaction plant adjusts its operating load after these two factors to a lower extent in comparison to the electrolyzer load which could be explained by two main reasons: the higher investment cost and the lower electricity consumption of the liquefaction process. The electrolyzer operates at an average load of 62-63% for Case 1, 2 and 3 despite the higher hydrogen demand in Case 2 and 3 which could indicate that a further increase of hydrogen demand would affect the average electrolyzer load minimally.

Another observation is the presence of compressor 1 in Case 3 where only liquid hydrogen is required, meaning that gaseous hydrogen is compressed up to 200 bar, stored in LRC and then liquefied. The model does however not take into consideration that the compressed hydrogen requires less energy to liquefy, meaning that compression up to 200 bar in Case 3 is an energy penalty. Still, compressor 1 is part of the cost optimal solution despite the energy losses related to both compression and storage of hydrogen. This could be explained by the model choosing to utilize the LRC in order to maintain a more constant inflow of hydrogen to the liquefaction plant.

It can be seen that trucks only appeared in the cost optimal solution for Case 1, where the trucks stood for approximately 0.08% of the yearly hydrogen demand and were utilized during 37 hours of the year. The trucks appeared during hours where there was a demand for compressed hydrogen while the electricity prices were low and thereby, the cable was already utilized at its maximum capacity. Trucks appeared also during hours when the electricity prices were high and thereby it was costly to produce hydrogen through the electrolyzer. The hydrogen price at the market would need to be increased above 178 €/MWh for the trucks to completely disappear, and if the market hydrogen price is less then 64 €/MWh, the pipeline appears in the cost optimal solution.

In the Theory Section 2.2.2, several safety concerns and regulations related to the implementation of wind turbines and solar PVs were described. More specifically, the concerns were regarding height, noise levels, electromagnetic radiation and light reflection. Wind turbines would most probably be a relevant technology only on the outer horizontal area where a 150 meters height limitation is in effect. However, the wind turbines which data was taken for from the Danish Energy Agency [57] have a height of 165 meters, but shorter wind turbines do exist, thus falling below the current height limitation of 150 meters in the outer horizontal area. Moreover, the required area for the installation of the solar PVs is large due to the low power produced per unit of area. This creates practical obstacles such as large land usage in connection to the airport. By taking into consideration the restrictions and difficulties regarding the local electricity generation via wind turbines and solar PVs, significant challenges are to be faced and the implementation of these technologies should be carefully examined with respect to the air traffic safety and the different national interests.

The largest storage option that the cost optimal solution includes for each case is LRC. This storage is located below ground and the surrounding solid rock should be able to withstand the high pressures. This project does however not take into account the geological conditions in connection to the airport, meaning that there is a possibility that the LRC storage will not be a viable option. If LRC storage is not allowed, the total system cost increases by 12% in Case 1, 7% in Case 2 and 2% in Case 3. Thus, the impact of no LRC is the lowest in a case where demand is met entirely by liquid hydrogen.

Moving forward, it would be beneficial if further research was done for year 2030, 2035, 2040 and 2045, thus taking into account the gradual construction of the cost-optimal system. Moreover, heat recovery at several technology units, such as the electrolyzer and compressors, could be implemented which would most probably result in energy-savings by integrating into Göteborg Landvetter Airport district heating system. Thus, the biofuel consumption for district heating could potentially be reduced and thereby decreasing the total system cost.

6

Conclusion

In this study, three cases representing the future demands for electricity and hydrogen at Göteborg Landvetter Airport were studied. The cases were based on different flight ranges and aviation fuels, including the use of batteries, compressed hydrogen and liquid hydrogen. The expected demand of hydrogen reaches up to 520 GWh (19 kton) in Case 1 and 680 GWh (21 kton) in Case 2 and 3. These estimations were done on basis of the current aviation traffic departing from Göteborg Landvetter Airport and should therefore be interpreted as an indication of the future demand, rather than a definitive value. Similarly, the expected demand of electricity is estimated to reach 30 GWh in Case 1.

The cost optimal solution for all the investigated cases includes onsite production via water electrolysis, which is highly dependent on the assumed electricity price. The required electricity in the system is best supplied by import of electricity via a cable connection and local electricity production via wind turbines and solar PVs, whereof the cable connection and the wind turbines are of most significant importance. There are however several challenges regarding safety concerns and practical obstacles related to wind turbines and solar PVs. Thus, their implementation should be carefully examined in future research studies. Moreover, the hydrogen storage that has the biggest impact on the total system cost, is the cryogenic hydrogen storage which allows the liquefaction plant to operate at maximum load for more hours during the year.

Gaseous hydrogen can be supplied at a marginal price of 53-54 €/MWh while liquid hydrogen can be supplied at a marginal price of 74-78 €/MWh. These price estimations are only valid for the investigated energy system of this project with the assumptions presented in the thesis.

References

[1] Masson-Delmotte, V., P. Zhai, H.-O. Pörtner, D. Roberts, J. Skea, P.R. Shukla, A. Pirani, W. Moufouma-Okia, C. Péan, R. Pidcock, S. Connors, J.B.R. Matthews, Y. Chen, X. Zhou, M.I. Gomis, E. Lonnoy, T. Maycock, M. Tignor, and T. Waterfield (eds.), Ed., *Global Warming of 1.5°C. An IPCC Special Report on the impacts of global warming of 1.5°C above pre-industrial levels and related global greenhouse gas emission pathways, in the context of strengthening the global response to the threat of climate change, sustainable development, and efforts to eradicate poverty*. Cambridge, UK and New York, NY, USA: Cambridge University Press, 2018, p. 616, https://doi.org/10.1017/9781009157940. DOI: 10.1017/9781009157940.

[2] F. Afonso, M. Sohst, C. M. Diogo, *et al.*, "Strategies towards a more sustainable aviation: A systematic review," *Progress in Aerospace Sciences*, vol. 137, p. 100 878, Feb. 2023, ISSN: 03760421. DOI: 10.1016/j.paerosci.2022.100878.

[3] *Års-och hållbarhetsredovisning 2023*, https://www.swedavia.se/globalassets/ahr/2024/swedavia-ars--och-hallbarhetsrapport-2023.pdf Accessed: 2024-05-09.

[4] *Års-och hållbarhetsredovisning 2022*. [Online]. Available: www.swedavia.se.

[5] *Miljö | göteborg landvetter airport*, https://www.swedavia.se/landvetter/miljo/ Accessed: 2024-01-17.

[6] *Swedavia höjer ambitionen i sitt klimatarbete ytterligare | göteborg landvetter airport*, https://www.swedavia.se/landvetter/nyheter/swedavia-hojer-ambitionen-i-sitt-klimatarbete-ytterligare/ Accessed: 2024-01-18.

[7] *Level 5 - airport carbon accreditation*, https://www.airportcarbonaccreditation.org/about/7-levels-of-accreditation/level-5/ Accessed: 2024-01-18.

[8] Fuel Cells and Hydrogen 2 Joint Undertaking, "Hydrogen-powered aviation – A fact-based study of hydrogen technology, economics, and climate impact by 2050," Publications Office, Tech. Rep., 2020. [Online]. Available: https://data.europa.eu/doi/10.2843/471510.

[9] E. Cabrera and J. M. M. de Sousa, "Use of sustainable fuels in aviation—a review," *Energies*, vol. 15, p. 2440, 7 Mar. 2022, ISSN: 1996-1073. DOI: 10.3390/en15072440.

[10] *Fact sheet 2 sustainable aviation fuel: Technical certification.* [Online]. Available: https://www.iata.org/contentassets/d13875e9ed784f75bac90f000760e998/saf-technical-certifications.pdf.

[11] NLR – Royal Netherlands Aerospace Centre and SEO Amsterdam Economics, *Destination 2050-a route to net zero european aviation preface*, 2021. [Online]. Available: https://www.destination2050.eu/wp-content/uploads/2021/03/Destination2050_Report.pdf.

[12] M. Prewitz, A. Bardenhagen, and R. Beck, "Hydrogen as the fuel of the future in aircrafts – challenges and opportunities," *International Journal of Hydrogen Energy*, vol. 45, pp. 25 378–25 385, 46 Sep. 2020, ISSN: 03603199. DOI: 10.1016/j.ijhydene.2020.06.238.

[13] J. Mukhopadhaya, "Performance analysis of fuel cell retrofit aircraft," Jul. 2023. [Online]. Available: https://theicct.org/wp-content/uploads/2023/08/Aircraft-retrofit-white-paper-A4-v3.pdf.

[14] J. R. Smith and E. Mastorakos, "An energy systems model of large commercial liquid hydrogen aircraft in a low-carbon future," *International Journal of Hydrogen Energy*, vol. 52, pp. 633–654, Jan. 2024, ISSN: 03603199. DOI: 10.1016/j.ijhydene.2023.04.039.

[15] J. Mukhopadhaya, "Performance analysis of evolutionary hydrogen-powered aircraft," Jan. 2022. [Online]. Available: https://theicct.org/wp-content/uploads/2022/01/LH2-aircraft-white-paper-A4-v4.pdf.

[16] M. El-Shafie, "Hydrogen production by water electrolysis technologies: A review," *Results in Engineering*, vol. 20, p. 101 426, Dec. 2023, ISSN: 25901230. DOI: 10.1016/j.rineng.2023.101426.

[17] Y. Wang, C. Wen, J. Tu, *et al.*, "The multi-scenario projection of cost reduction in hydrogen production by proton exchange membrane (pem) water electrolysis in the near future (2020–2060) of china," *Fuel*, vol. 354, p. 129 409, Dec. 2023, ISSN: 00162361. DOI: 10.1016/j.fuel.2023.129409.

[18] A. Arsad, M. Hannan, A. Q. Al-Shetwi, *et al.*, "Hydrogen electrolyser technologies and their modelling for sustainable energy production: A comprehensive review and suggestions," *International Journal of Hydrogen Energy*, vol. 48, pp. 27 841–27 871, 72 Aug. 2023, ISSN: 03603199. DOI: 10.1016/j.ijhydene.2023.04.014.

[19] M. Balat, "Potential importance of hydrogen as a future solution to environmental and transportation problems," *International Journal of Hydrogen Energy*, vol. 33, pp. 4013–4029, 15 Aug. 2008, ISSN: 03603199. DOI: 10.1016/j.ijhydene.2008.05.047.

[20] K. Ohmstede, C. Thies, A. Barke, and T. S. Spengler, "Evaluation of hydrogen supply options for sustainable aviation," in 2023, pp. 27–42. DOI: 10.1007/978-3-031-38145-4_2.

[21] Danish Energy Agency and Energine, "Technology data for renewable fuels," 2024. [Online]. Available: http://www.ens.dk/teknologikatalog.

[22] M. Holst, S. Aschbrenner, T. Smolinka, C. Voglstätter, and G. Grimm, "Cost forecast for low temperature electrolysis - technology driven bottom-up prognosis for pem and alkaline water electrolysis systems," 2021. [Online]. Available: https://www.ise.fraunhofer.de/content/dam/ise/de/documents/publications/studies/cost-forecast-for-low-temperature-electrolysis.pdf.

[23] Danish Energy Agency and Energinet, "Technology Data Renewable fuels," 2021. [Online]. Available: http://www.ens.dk/teknologikatalog.

[24] A. V. Zhuzhgov, O. P. Krivoruchko, L. A. Isupova, O. N. Mart'yanov, and V. N. Parmon, "Low-temperature conversion of ortho-hydrogen into liquid para-hydrogen: Process and catalysts. review," *Catalysis in Industry*, vol. 10, pp. 9–19, 1 Jan. 2018, ISSN: 2070-0504. DOI: 10.1134/S2070050418010117.

[25] T. Zhang, J. Uratani, Y. Huang, L. Xu, S. Griffiths, and Y. Ding, "Hydrogen liquefaction and storage: Recent progress and perspectives," *Renewable and Sustainable Energy Reviews*, vol. 176, p. 113 204, Apr. 2023, ISSN: 13640321. DOI: 10.1016/j.rser.2023.113204.

[26] E. Connelly, M. Penev, A. Elgowainy, and C. Hunter, *Current status of hydrogen liquefaction costs*, Sep. 2019. [Online]. Available: https://www.hydrogen.energy.gov/docs/hydrogenprogramlibraries/pdfs/19001_hydrogen_liquefaction_costs.pdf?Status=Master.

[27] Amgad Elgowainy and Krishna Reddi, Argonne National Laboratory, "Hydrogen Delivery Scenario Analysis Model (HDSAM)," version 4.5, 2024. [Online]. Available: https://hdsam.es.anl.gov/.

[28] H. W. Langmi, N. Engelbrecht, P. M. Modisha, and D. Bessarabov, "Hydrogen storage," in Elsevier, 2022, pp. 455–486. DOI: 10.1016/B978-0-12-819424-9.00006-9.

[29] F. Ghaffari-Tabrizi, J. Haemisch, and D. Lindner, "Reducing hydrogen boil-off losses during fuelling by pre-cooling cryogenic tank," *Hydrogen*, vol. 3, pp. 255–269, 2 Jun. 2022, ISSN: 2673-4141. DOI: 10.3390/hydrogen3020015.

[30] Lutz Decker, "Liquid Hydrogen Distribution Technology," 2019. [Online]. Available: https://www.sintef.no/globalassets/project/hyper/presentations-day-2/day2_1105_decker_liquid-hydrogen-distribution-technology_linde.pdf.

[31] J. Fesmire, A. Swanger, J. Jacobson, and W. Notardonato, "Energy efficient large-scale storage of liquid hydrogen," *IOP Conference Series: Materials Science and Engineering*, vol. 1240, 1 May 2022, ISSN: 1757-8981. DOI: 10.1088/1757-899X/1240/1/012088.

[32] Danish Energy Agency and Energinet, "Technology Data Energy storage," 2018. [Online]. Available: http://www.ens.dk/teknologikatalog.

[33] Y. K. Patanwar, H.-M. Kim, D. Deb, and Y. K. Gujjala, "Underground storage of hydrogen in lined rock caverns: An overview of key components and hydrogen embrittlement challenges," *International Journal of Hydrogen Energy*, vol. 50, pp. 116–133, Jan. 2024, ISSN: 03603199. DOI: 10.1016/j.ijhydene.2023.08.342.

[34] D. Papadias and R. Ahluwalia, "Bulk storage of hydrogen," *International Journal of Hydrogen Energy*, vol. 46, pp. 34 527–34 541, 70 Oct. 2021, ISSN: 03603199. DOI: 10.1016/j.ijhydene.2021.08.028.

[35] M. Masoudi, A. Hassanpouryouzband, H. Hellevang, and R. S. Haszeldine, "Lined rock caverns: A hydrogen storage solution," *Journal of Energy Storage*, vol. 84, p. 110 927, Apr. 2024, ISSN: 2352152X. DOI: 10.1016/j.est.2024.110927.

[36] O. Kruck, F. Crotogino, R. Prelicz, and T. Rudolph, "Overview on all known underground storage technologies for hydrogen," 2013. [Online]. Available: https://www.hyunder.eu/wp-content/uploads/2016/01/D3.1_Overview-of-all-known-underground-storage-technologies.pdf.

[37] K. Law, J. Rosenfeld, V. Han, M. Chan, H. Chiang, and J. Leonard, *Hydrogen storage cost analysis*, Mar. 2013. DOI: 10.2172/1082754.

[38] C. Houchins, B. D. James, Y. Acevedo, and Z. Watts, *Hydrogen storage system cost analysis (2017-2021)*, Sep. 2022. [Online]. Available: https://www.osti.gov/servlets/purl/1975554.

[39] S. S. Makridis, "Hydrogen storage and compression," in Institution of Engineering and Technology, Jul. 2016, pp. 1–28. DOI: 10.1049/PBPO101E_ch1.

[40] Danish Energy Agency and Energinet, "Technology Data Energy Transport," 2021. [Online]. Available: https://ens.dk/sites/ens.dk/files/Analyser/technology_data_for_energy_transport.pdf.

[41] P. Preuster, A. Alekseev, and P. Wasserscheid, "Hydrogen storage technologies for future energy systems," *Annual Review of Chemical and Biomolecular Engineering*, vol. 8, pp. 445–471, 1 Jun. 2017, ISSN: 1947-5438. DOI: 10.1146/annurev-chembioeng-060816-101334.

[42] B. C. Tashie-Lewis and S. G. Nnabuife, "Hydrogen production, distribution, storage and power conversion in a hydrogen economy - a technology review," *Chemical Engineering Journal Advances*, vol. 8, p. 100 172, Nov. 2021, ISSN: 26668211. DOI: 10.1016/j.ceja.2021.100172.

[43] C. Tsiklios, M. Hermesmann, and T. Müller, "Hydrogen transport in large-scale transmission pipeline networks: Thermodynamic and environmental assessment of repurposed and new pipeline configurations," *Applied Energy*, vol. 327, p. 120 097, Dec. 2022, ISSN: 03062619. DOI: 10.1016/j.apenergy.2022.120097.

[44] J. R. Fekete, J. W. Sowards, and R. L. Amaro, "Economic impact of applying high strength steels in hydrogen gas pipelines," *International Journal of Hydrogen Energy*, vol. 40, pp. 10 547–10 558, 33 Sep. 2015, ISSN: 03603199. DOI: 10.1016/j.ijhydene.2015.06.090.

[45] Danish Energy Agency and Energinet, "Technology Data Sheet Transport of Energy," version 4, 2023. [Online]. Available: https://ens.dk/sites/ens.dk/files/Analyser/energy_transport_datasheet.xlsx.

[46] A. Kumar, R. Padmanaban, V. Sanghi, and H. Shah, "Powering the future of electric aviation tanay dalmia defne doken," 2022. [Online]. Available: http://www.sti.nasa.gov.

[47] J. Mukhopadhaya and B. Graver, "Performance analysis of regional electric aircraft," Jul. 2022. [Online]. Available: https://theicct.org/wp-content/uploads/2022/07/global-aviation-performance-analysis-regional-electric-aircraft-jul22-1.pdf-1.pdf.

[48] G. Zubi, R. Dufo-López, M. Carvalho, and G. Pasaoglu, "The lithium-ion battery: State of the art and future perspectives," *Renewable and Sustainable Energy Reviews*, vol. 89, pp. 292–308, Jun. 2018, ISSN: 13640321. DOI: 10.1016/j.rser.2018.03.002.

[49] *Easy access rules for aerodromes (regulation (eu) no 139/2014)*, https://www.easa.europa.eu/en/downloads/98016/en Accessed: 2024-05-07, Jun. 2023.

[50] "Mitigating wind turbine radar interference," https://www.energy.gov/eere/wind/mitigating-wind-turbine-radar-interference Accessed: 2024-05-07.

[51] A. Anurag, J. Zhang, J. Gwamuri, and J. M. Pearce, "General design procedures for airport-based solar photovoltaic systems," *Energies*, vol. 10, p. 1194, 8 Aug. 2017, ISSN: 1996-1073. DOI: 10.3390/en10081194.

[52] S. Öberg, M. Odenberger, and F. Johnsson, "The cost dynamics of hydrogen supply in future energy systems – a techno-economic study," *Applied Energy*, vol. 328, p. 120 233, Dec. 2022, ISSN: 03062619. DOI: 10.1016/j.apenergy.2022.120233.

[53] I. Staffell and S. Pfenninger, "Using bias-corrected reanalysis to simulate current and future wind power output," *Energy*, vol. 114, pp. 1224–1239, Nov. 2016, ISSN: 03605442. DOI: 10.1016/j.energy.2016.08.068.

[54] S. Pfenninger and I. Staffell, "Long-term patterns of european pv output using 30 years of validated hourly reanalysis and satellite data," *Energy*, vol. 114, pp. 1251–1265, Nov. 2016, ISSN: 03605442. DOI: 10.1016/j.energy.2016.08.060.

[55] *Renewables ninja*, www.renewables.ninja Accessed: 2024-01-29.

[56] B. Lux and B. Pfluger, "A supply curve of electricity-based hydrogen in a decarbonized european energy system in 2050," *Applied Energy*, vol. 269, p. 115 011, Jul. 2020, ISSN: 03062619. DOI: 10.1016/j.apenergy.2020.115011.

[57] Danish Energy Agency and Energinet, "Technology Data Sheet Renewable fuels," version 10, 2021. [Online]. Available: https://ens.dk/sites/ens.dk/files/Analyser/version_10_-_data_sheets_for_renewable_fuels.xlsx.

[58] "Taxa för härryda kommuns allmänna vatten-och avloppsanläggning," 2023. [Online]. Available: https://hvaa.se/download/18.1abb884718c8ab9a9f739ec8/1705325518506/Taxa%20f%C3%B6r%20vattentj%C3%A4nster%202024.pdf.

[59] J. André, S. Auray, D. D. Wolf, M.-M. Memmah, and A. Simonnet, "Time development of new hydrogen transmission pipeline networks for France," *International Journal of Hydrogen Energy*, vol. 39, pp. 10 323–10 337, 20 Jul. 2014, ISSN: 03603199. DOI: 10.1016/j.ijhydene.2014.04.190.

[60] Härryda Energi, *Elnätspriser*, https://harrydaenergi.se/elnat/elnatspriser/, Accessed: 2024-03-11.

[61] Danish Energy Agency and Energinet, "Technology Data Sheet Energy Storage," version 7, 2023. [Online]. Available: https://ens.dk/sites/ens.dk/files/Analyser/technology_datasheet_for_energy_storage.xlsx.

[62] Danish Energy Agency and Energinet, "Technology Data Sheet Generation of Electricity and District Heating," version 12, 2023. [Online]. Available: https://ens.dk/sites/ens.dk/files/Analyser/version_12_-_technology_data_for_el_and_dh.xlsx.

[63] P. George, B. Robert, C. John, and R. Robert, *Hydrogen station compression, storage, and dispensing technical status and costs*, May 2014. [Online]. Available: https://www.nrel.gov/docs/fy14osti/58564.pdf.

[64] R. Ahluwalia, T. Hua, and J. Peng, "On-board and off-board performance of hydrogen storage options for light-duty vehicles," *International Journal of Hydrogen Energy*, vol. 37, pp. 2891–2910, 3 Feb. 2012, ISSN: 03603199. DOI: 10.1016/j.ijhydene.2011.05.040.

[65] J. W. Leachman, R. T. Jacobsen, S. G. Penoncello, and E. W. Lemmon, "Fundamental equations of state for parahydrogen, normal hydrogen, and orthohydrogen," *Journal of Physical and Chemical Reference Data*, vol. 38, pp. 721–748, 3 Sep. 2009, ISSN: 0047-2689. DOI: 10.1063/1.3160306.

[66] B. Lukasik and W. Wisniowski, "All-electric propulsion for future business jet aircraft: A feasibility study," *Proceedings of the Institution of Mechanical Engineers, Part G: Journal of Aerospace Engineering*, vol. 231, pp. 2203–2213, 12 Oct. 2017, ISSN: 0954-4100. DOI: 10.1177/0954410017727027.

[67] M. Z. Sogut, Ö. Seçgin, and S. Ozkaynak, "Investigation of thermodynamics performance of alternative jet fuels based on decreasing threat of paraffinic and sulfur," *Energy*, vol. 181, pp. 1114–1120, Aug. 2019, ISSN: 03605442. DOI: 10.1016/j.energy.2019.05.136.

A

Efficiencies

Table A.1: Efficiencies for battery-electric [66] and JET-engine [67].

$\eta_{JetEngine}$	0.37
η_{EM}	0.98
$\eta_{Electronics}$	0.96
η_{Dist}	0.98
$\eta_{Management}$	0.98

B

Costs: Liquefaction & Cryogenic Tank

The cost for the liquefaction process is based on the cost function from the HDSAM model [27] presented in Equation B.1. Here, the cost is obtained in [US$] while the capacity ($Cap_{Liq}$) is given in tonnes per day (tpd). Moreover, I is the Chemical Engineering Plant Cost Index (CEPCI) value.

$$Installed\ Liquefier\ Capital\ Cost = 5.6 \cdot 10^6 \cdot Cap_{Liq}^{0.8} \cdot I \tag{B.1}$$

The function was plotted on Excel for capacities between 20 tpd up to 200 tpd and a linear regression was preformed resulting in Equation B.2, where capacity should be inserted in megawatts and the liquefier cost ($C^{Liquefier}$) is obtained in €. The total capital investment investment cost (C_{Liq}^{CAPEX}) given in Equation B.4 included also Owner's costs (C^{Owner}) which were calculated by using Equation B.3. Owner's cost account for the additional investment required for engineering, further research studies and legal fees related to construction [26]. Similar expenses are also taken into account for other technologies.

$$C^{Liquefier} = 1600000 \cdot Cap_{Liq} + 46000000 \tag{B.2}$$

$$C^{Owner} = 0.12 \cdot C^{Liquefier} \tag{B.3}$$

$$C_{Liq}^{CAPEX} = C^{Liquefier} + C^{Owner} \tag{B.4}$$

The cost for the cryogenic tank for storage of liquid hydrogen was based on the cost function estimated by the HDSAM model [27], presented in Equation B.5 where V_{LH_2Tank} and $Cost$ are expressed in terms of m^3 and [US$$_{2016}$] respectively.

$$Cost = 3100 \cdot V_{LH_2Tank} + 5646600 \tag{B.5}$$

This equation was plotted in Excel for storage capacities between 50 t and 250 t and a linear regression with interception through zero was performed resulting in Equation B.6, where the cost of the cryogenic tank ($C^{Equipment}$) is obtained in €. Additionally, other capital costs (C^{Other}) were estimated by using Equation B.7 and took into account costs for site preparation, engineering & design, project contingency, up-front permitting and owner's costs. Finally, an average of the balance of plant cost (C^{BOP}) was calculated within the same range of storage capacities and was expressed

in terms of the capital investment cost for the cryogenic tank as shown in Equation B.8.

$$C^{Equipment} = 930 \cdot Cap_{LH_2Tank} \tag{B.6}$$

$$C^{Other} = 0.40 \cdot C^{Equipment} \tag{B.7}$$

$$C^{BOP} = 0.045 \cdot (C^{Equipment} + C^{Other}) \tag{B.8}$$

Note that the two functions that were obtained via linear progression, already took into account inflation and conversion from American dollar to Euro.

C

Load Duration Curves

The following section presents the load duration curves for the electricity import and export as well as for compressor 1 & 2.

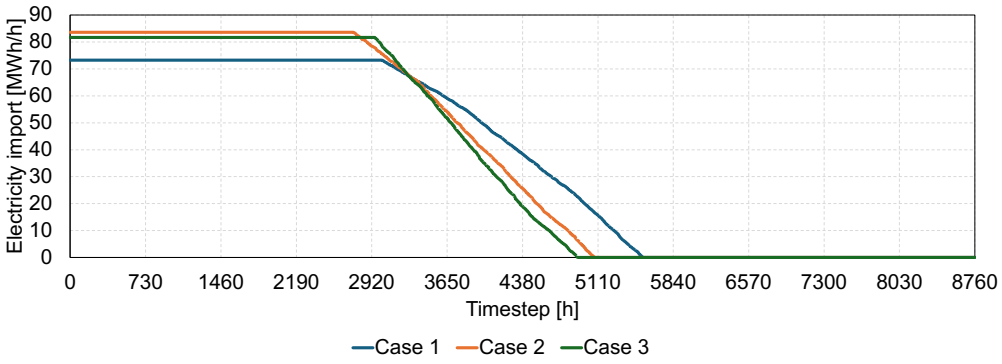

Figure C.1: Load duration curve for electricity import for Case 1, 2 & 3.

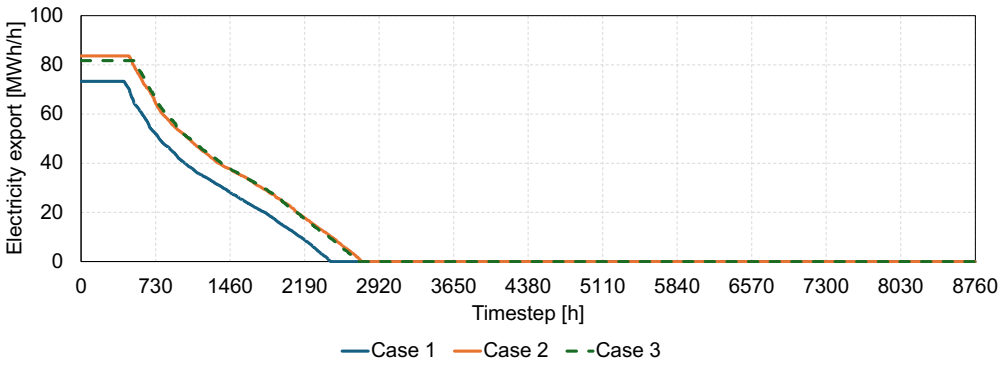

Figure C.2: Load duration curve for electricity export for Case 1, 2 & 3.

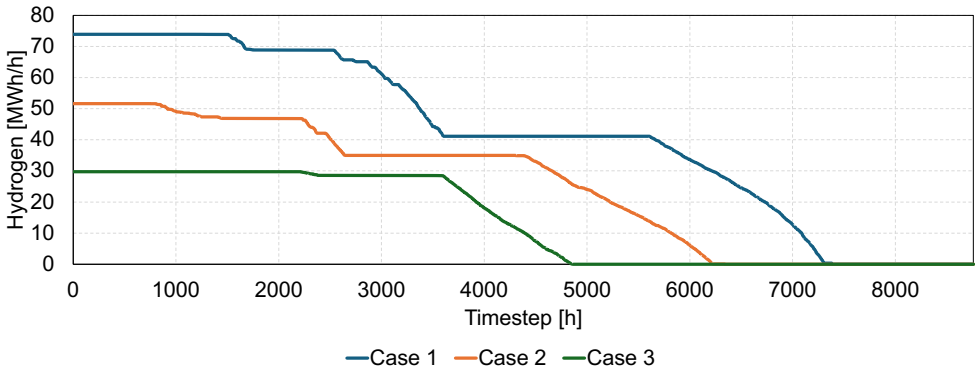

Figure C.3: Load duration curve for hydrogen output from compressor 1 for Case 1, 2 & 3.

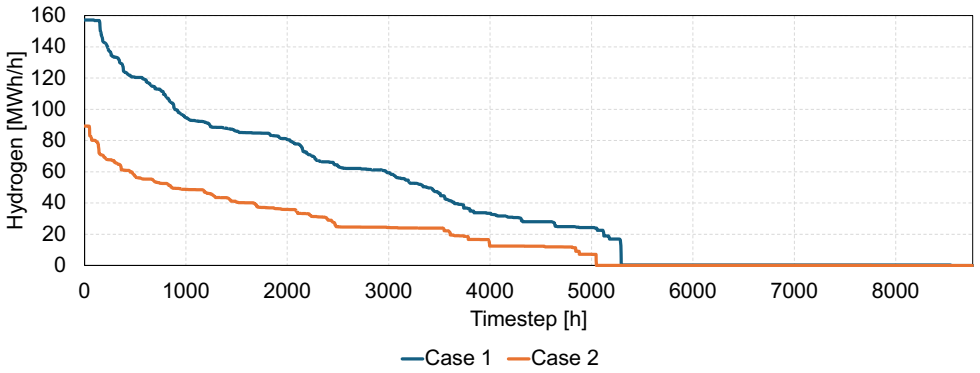

Figure C.4: Load duration curve for hydrogen output from compressor 2 for Case 1 & 2.

D

Sensitivity Analysis: Capacities

In this appendix the results from single and double are presented for the remaining cases.

D.1 Single Limitations

The following section presents installed capacities for the technology and storage units for single limitations.

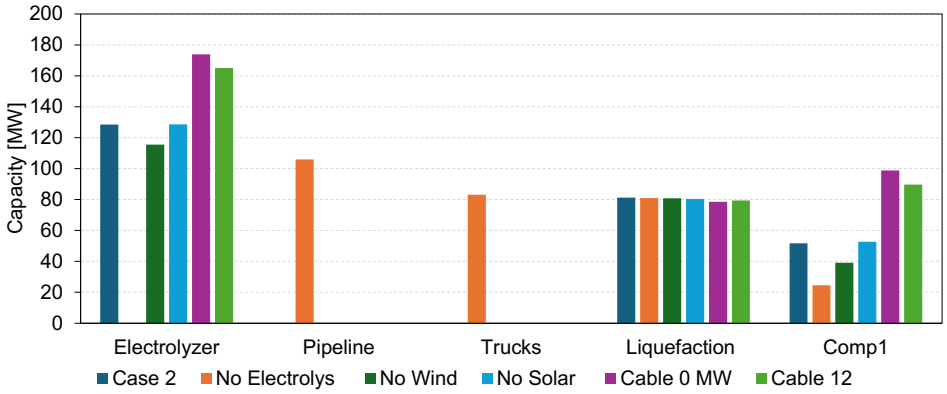

Figure D.1: The effect of single limitations on the installed capacity of technology units in Case 2.

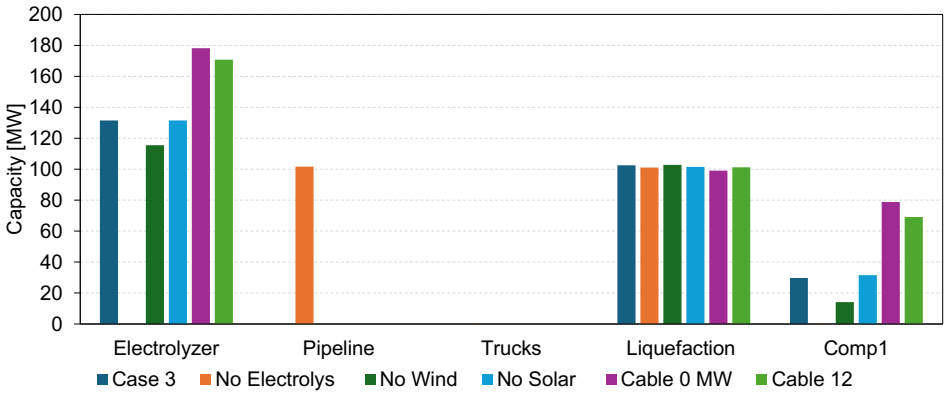

Figure D.2: The effect of single limitations on the installed capacity of technology units in Case 3.

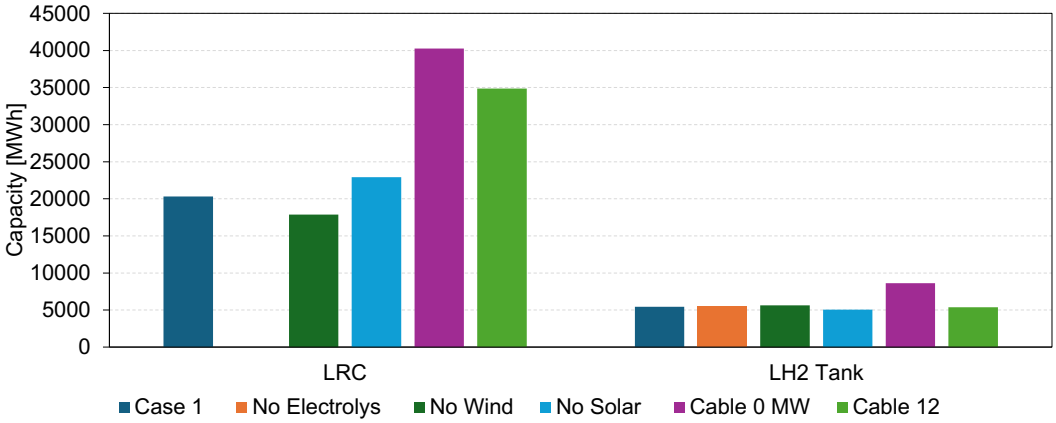

Figure D.3: The effect of single limitations on the installed capacity of the LRC and cryogenic tank in Case 1.

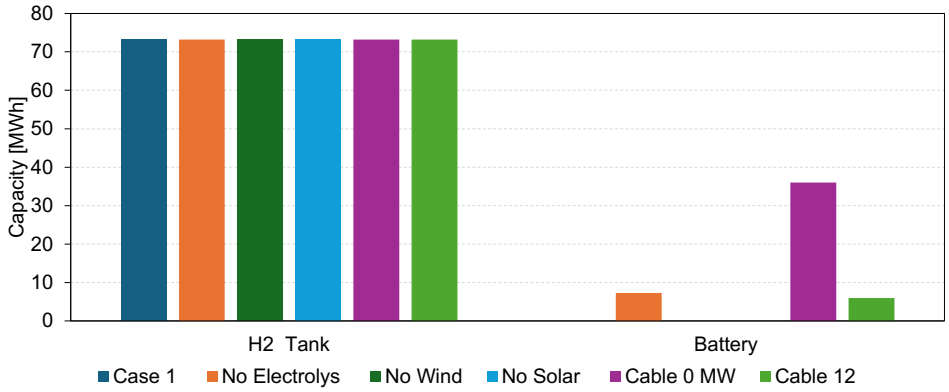

Figure D.4: The effect of single limitations on the installed capacity of the battery storage and pressurized vessel in Case 2.

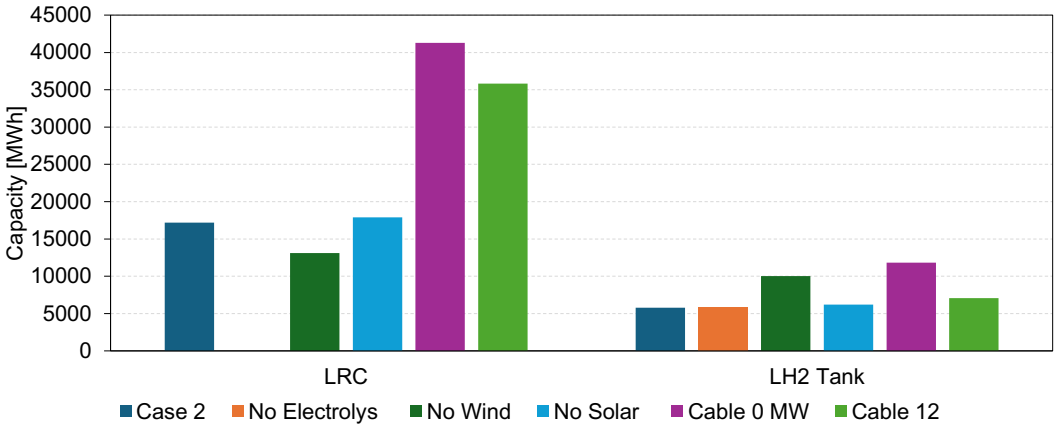

Figure D.5: The effect of single limitations on the installed capacity of the LRC and cryogenic tank in Case 2.

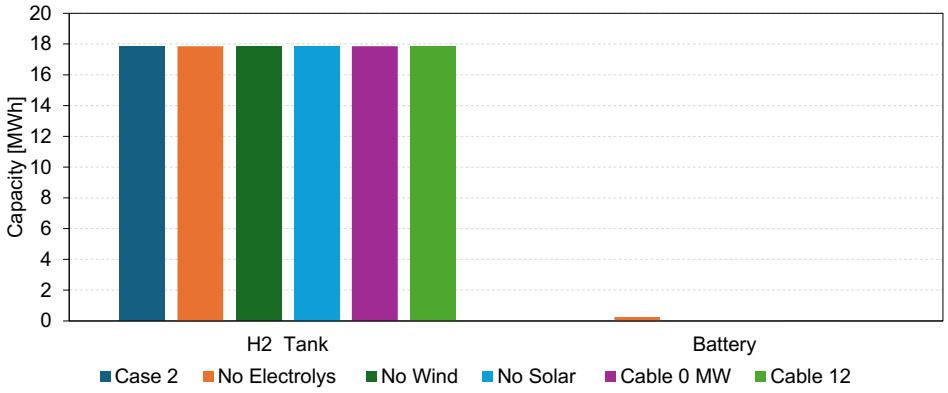

Figure D.6: The effect of single limitations on the installed capacity of the battery storage and pressurized vessel in Case 2.

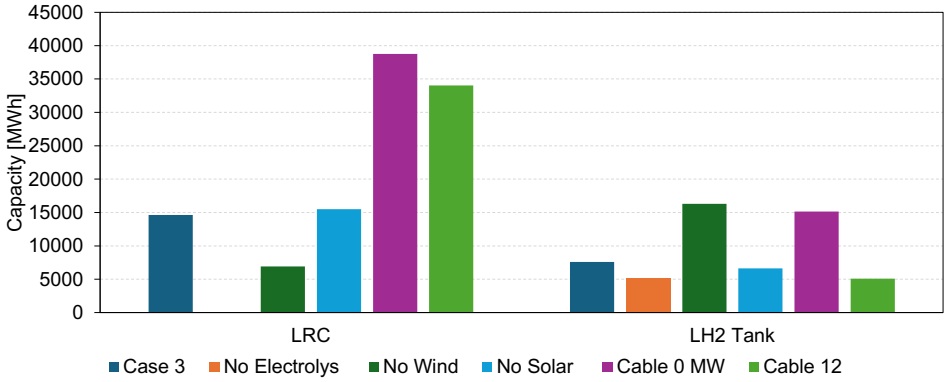

Figure D.7: The effect of single limitations on the installed capacity of the LRC and cryogenic tank in Case 3.

D.2 Double Limitations

The following section presents installed capacities for technologies and storage for double limitations.

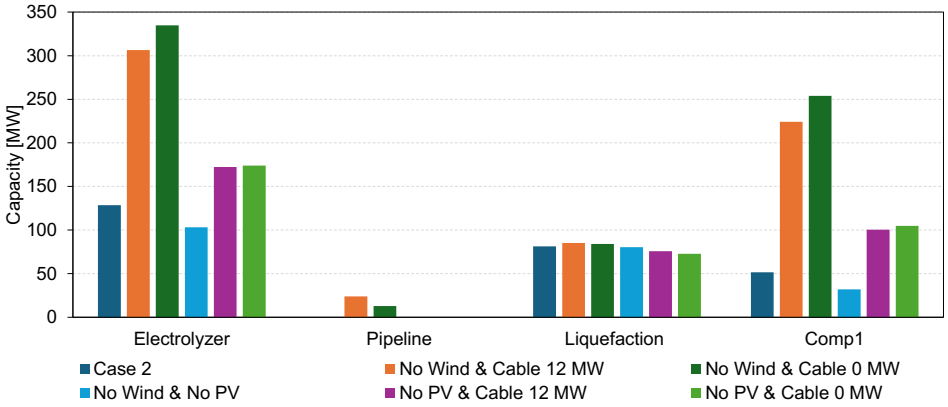

Figure D.8: The effect of double limitations on the installed capacity of technology units in Case 2.

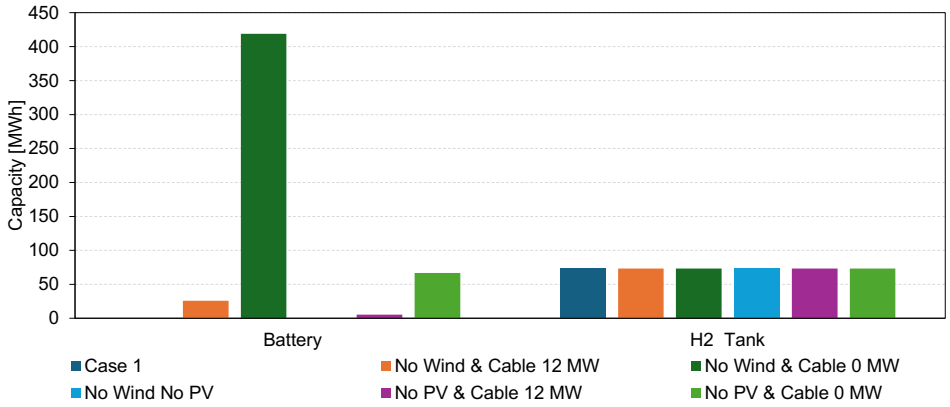

Figure D.11: The effect of double limitations on the installed capacity of the battery and pressurized vessel in Case 1.

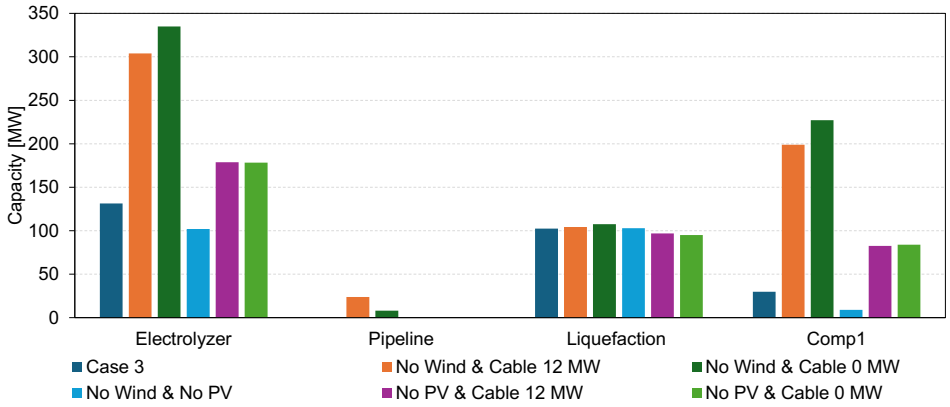

Figure D.9: The effect of double limitations on the installed capacity of technology units in Case 3.

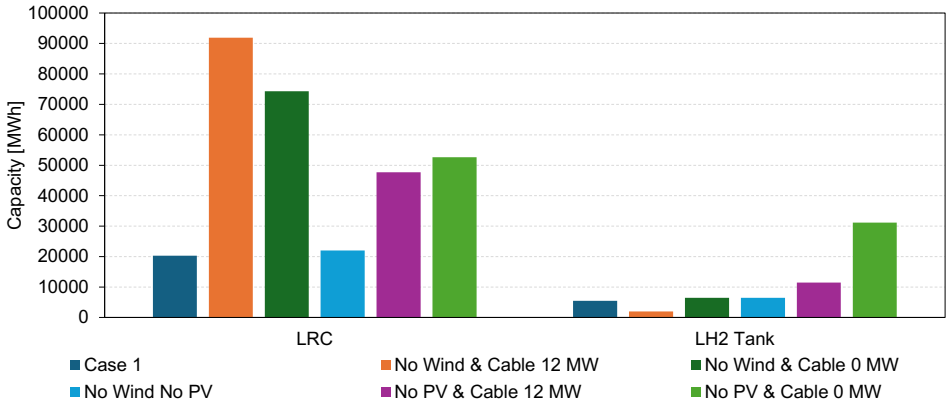

Figure D.10: The effect of double limitations on the installed capacity of the LRC and cryogenic tank in Case 1.

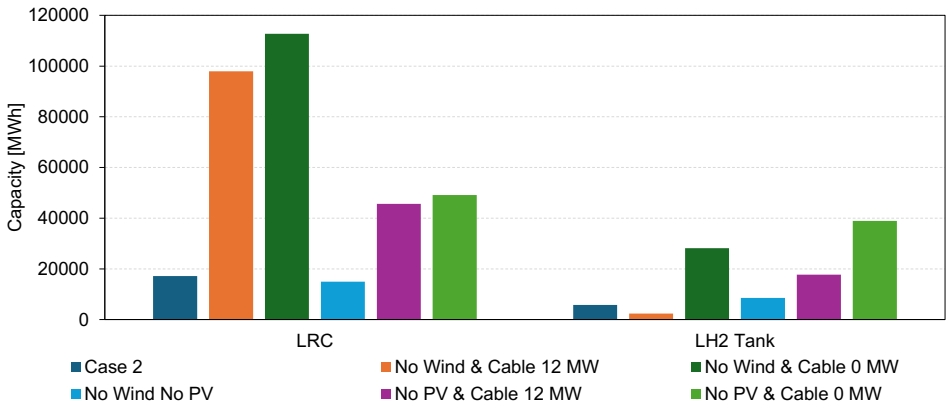

Figure D.12: The effect of double limitations on the installed capacity of the LRC and cryogenic tank in Case 2.

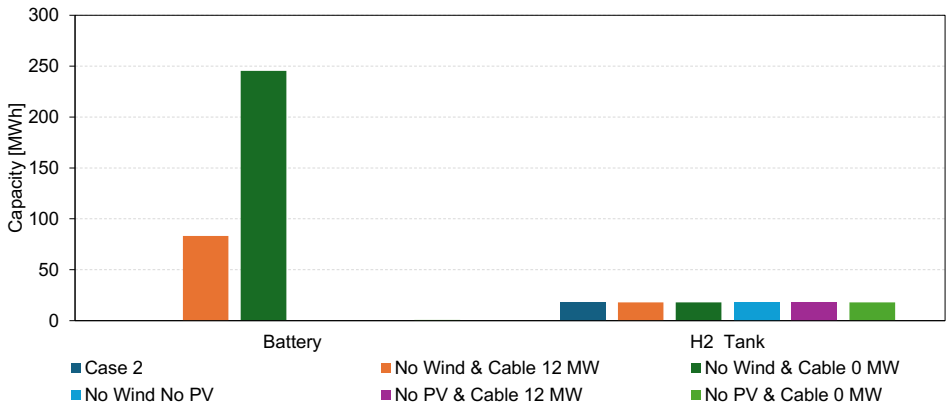

Figure D.13: The effect of double limitations on the installed capacity of the battery and pressurized vessel in Case 2.

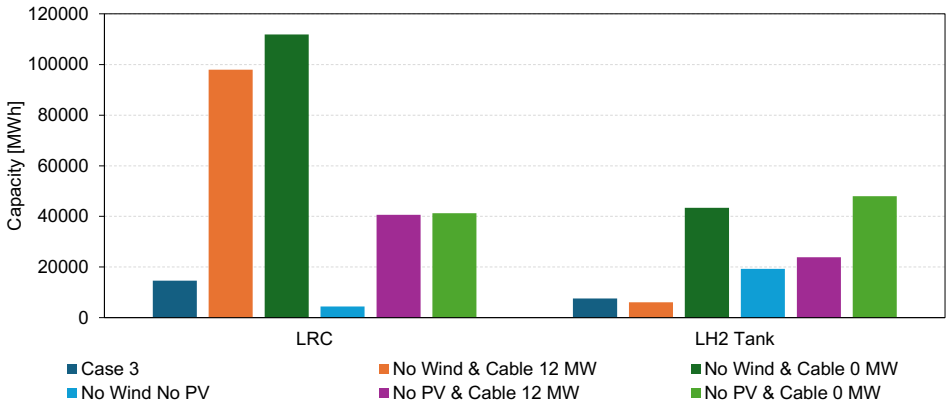

Figure D.14: The effect of double limitations on the installed capacity of the LRC and cryogenic tank in Case 3.

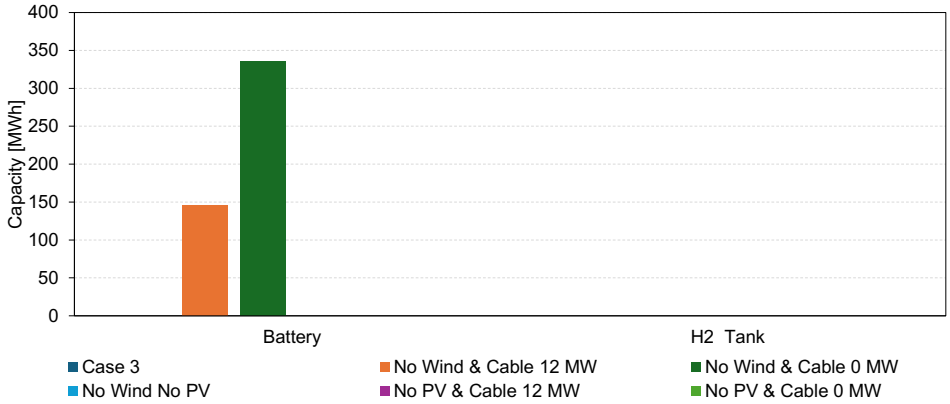

Figure D.15: The effect of double limitations on the installed capacity of the battery and pressurized vessel in Case 3.

E

Electricity Supply and Consumption

In this appendix the electricity supply and demand can be seen individually for 8 days in January.

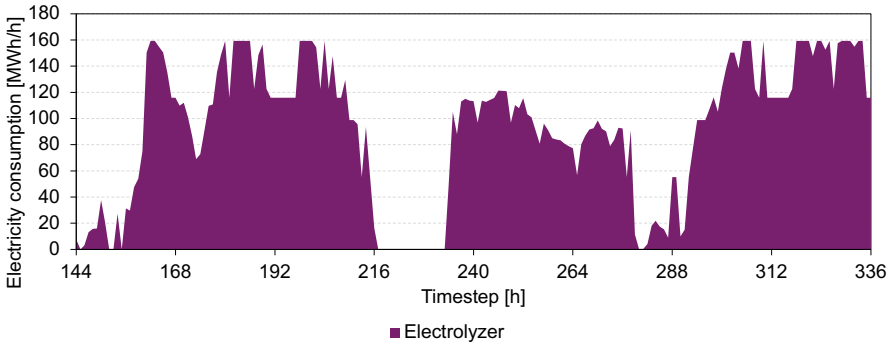

Figure E.1: The electricity consumption of the electrolyzer for 8 days in January.

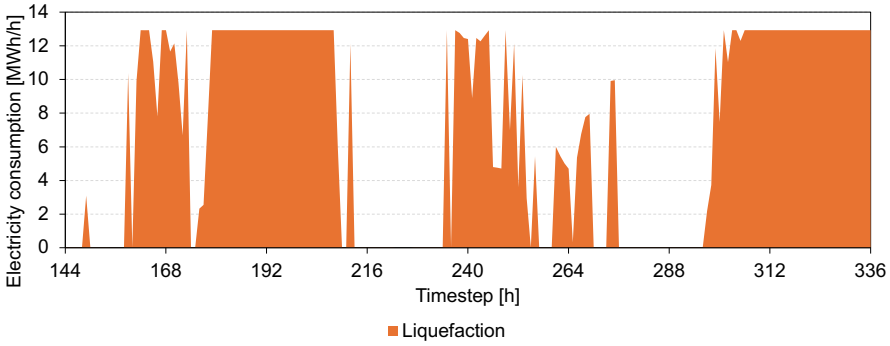

Figure E.2: The electricity consumption of the liquefaction plant.

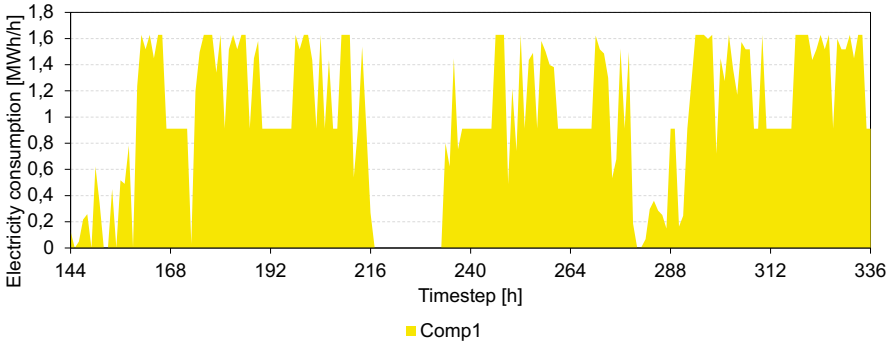

Figure E.3: The electricity consumption of compressor 1.

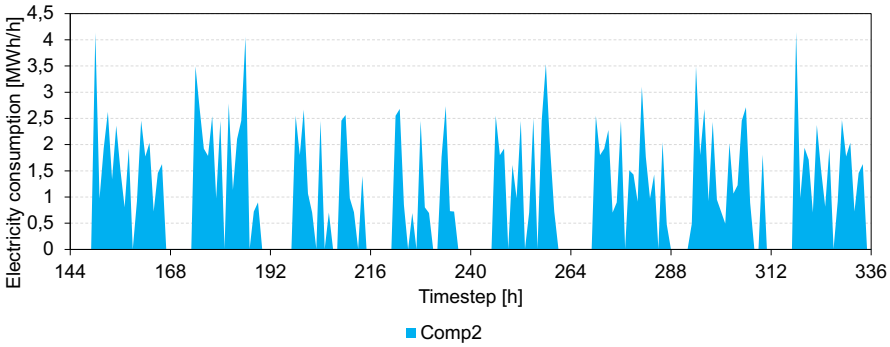

Figure E.4: The electricity consumption of compressor 2.

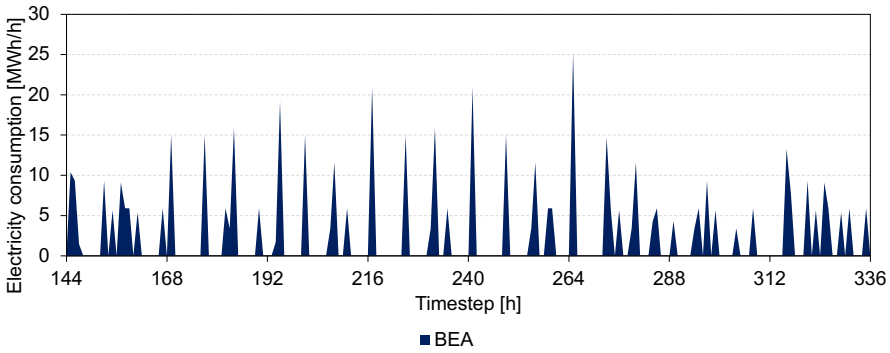

Figure E.5: The electricity consumption by the battery-electric aircraft.

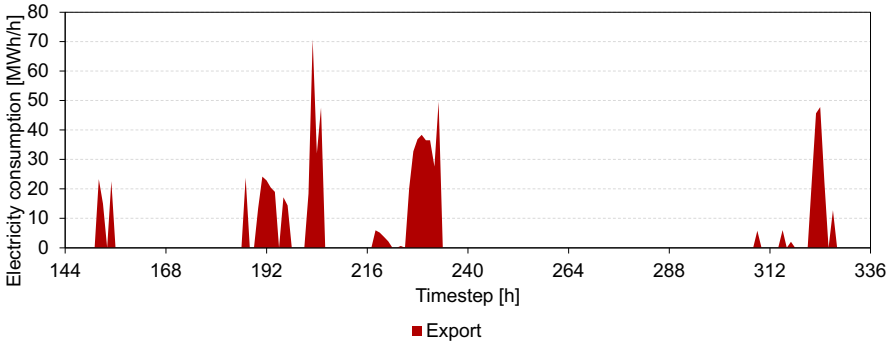

Figure E.6: The electricity exported to the grid.

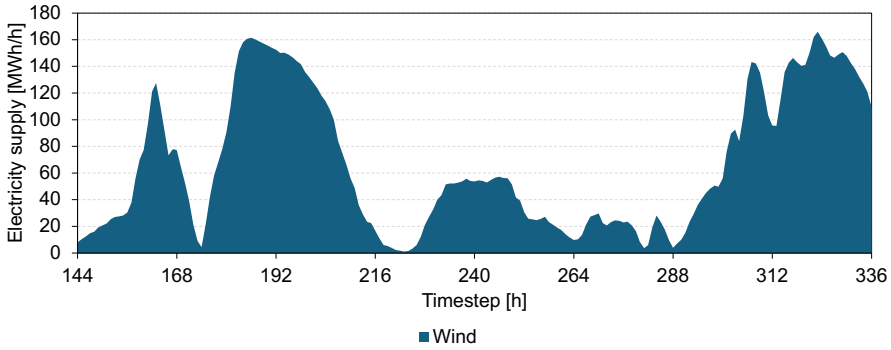

Figure E.7: The electricity supply from local wind turbines.

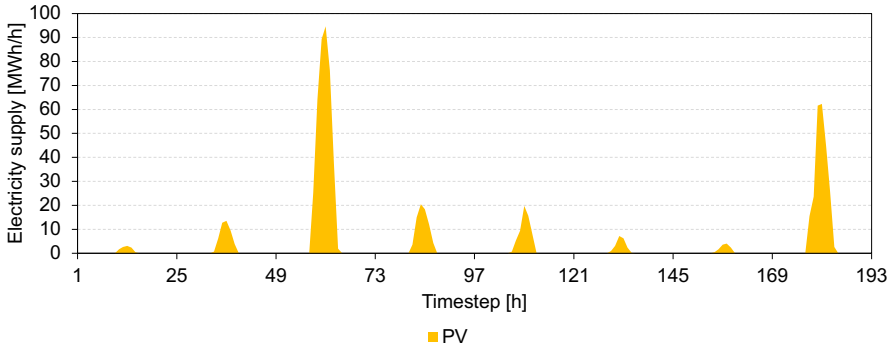

Figure E.8: The electricity supplied from local solar PVs.

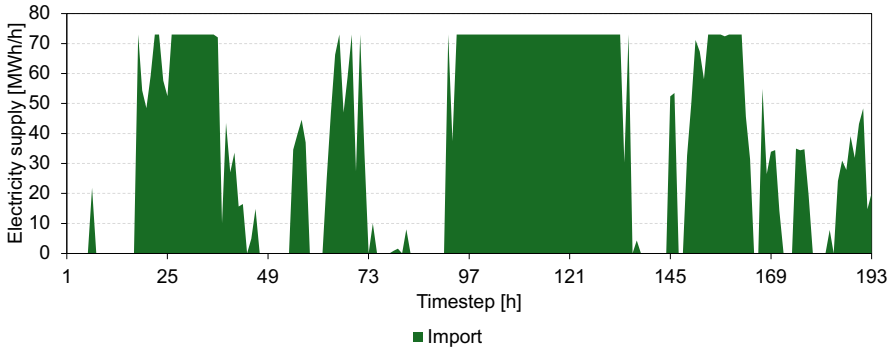

Figure E.9: The electricity supplied from the grid.

DEPARTMENT OF SPACE, EARTH AND ENVIRONMENT
CHALMERS UNIVERSITY OF TECHNOLOGY
Gothenburg, Sweden
www.chalmers.se

CHALMERS
UNIVERSITY OF TECHNOLOGY